

ABSTRACT

Characterization of the Low pH sensing dye, LysoSensor Yellow/Blue DND-160, under High Hydrostatic Pressures

By Hector Michael Belleza de Pedro

DND-160, a low-pH probe dye, was characterized under high hydrostatic pressures in pH buffers acetate ($pK_a = 4.8$), MOPS ($pK_a = 7.2$) and BES ($pK_a = 7.1$). The effect of pressurization on the fluorescence of DND-160 shows differences compared to previously studied near-neutral pH seminaphthorhodafluor (SNARF) and seminaphthofluorescein (SNAFL) dyes, including a pressure sensitivity of the deprotonated emission and a buffer solvent dependent ΔV of the acid-base reaction for DND-160. The ΔV was determined from the pressure dependence of the equilibrium constant pK_a , calculated from the fluorescence of the dye at different pH. The ΔV of DND-160 in acetate was about half of the value in MOPS and BES. We hypothesize that the differences in DND-160 pressure response compared to previously studied dyes are due to the differences in their fluorescence mechanism. C.SNAFL and C.SNARF emission is solely dependent on the superposition of the fluorescence of its two dye forms, i.e., the protonated and deprotonated forms, while DND-160 emission depends on two factors, the concentration of the two chemical forms and on the interaction of its locally-excited and charge transfer states.

Characterization of the Low pH Sensing Dye, LysoSensor Yellow/Blue DND-160, under
High Hydrostatic Pressures

A Thesis

Submitted to the
Faculty of Miami University
in partial fulfillment of
the requirements for the degree of
Master of Science
Department of Physics

by

Hector Michael Belleza de Pedro

Miami University

Oxford, Ohio

2008

Advisor _____
(Paul Urayama)

Reader _____
(William Houk)

Reader _____
(Douglas Marcum)

Table of Contents

Table of Contents.....	ii
List of Tables.....	iii
List of Figures.....	iv
List of Abbreviation.....	vi
Chapter I: Introduction.....	1
Goals.....	6
Chapter II: Fluorescence Spectroscopy.....	7
Overview.....	7
Fluorescence.....	7
Solvent Relaxation.....	10
Fluorescence Measurements.....	13
pH Sensing.....	14
Two State Model.....	15
Fluorescence pH Sensing under High Pressure.....	16
Chapter III: Instrumentation.....	18
Overview.....	18
Sample Preparation.....	18
Instrumentation.....	19
Data Collection.....	22
Chapter IV: Results and Discussions.....	27
Overview.....	27
Buffer Characterization.....	27
DND-160 Results.....	33
Fluorescence Emission.....	34
ΔV Calculations.....	40
Discussions.....	42
Chapter V: Conclusions.....	47
References.....	50

List of Tables

Table 1.1	ΔV of some chemical reactions	2
Table 1.2	List of some pH values of organelles/cells	3
Table 1.3.	List of some pH dyes	5
Table 3.2	Intensity wavelength window	23
Table 4.1	pKa and ΔV of C.SNAFL and C.SNARF	28
Table 4.2	ΔV of pH buffers	33
Table 4.3	pKa values of DND-160	36
Table 4.4	ΔV of DND-160 in different buffers	41

List of Figures

Figure 1.1	The “pump and the leak” model for maintaining intracellular pH	3
Figure 2.1	Simplified version of a Jablonski diagram	8
Figure 2.2	Absorption and Emission Spectra of Quinine sulfate in water	9
Figure 2.3	Jablonski diagram with FRET and quenching	10
Figure 2.4	Jablonski diagram with specific environmental effects on the excited state	11
Figure 2.5	Solvent polarity dependence of a polar probe’s charge transfer state	12
Figure 2.6	Emission spectra of Dapoxyl SEDA in different solvents with increasing polarity	13
Figure 2.7	Fluorescence emission of pH sensing probes at different pH	14
Figure 3.1	Chemical structures of pH sensing dyes	18
Figure 3.2	Schematic diagram of the Experimental Setup	20
Figure 3.3	High Pressure Chamber and Lens Setup	21
Figure 3.4	Fluorescence of DND-160 in its low and high pH form	22
Figure 3.5	Background spectrum and low pH fluorescence of DND-160 in MOPS	24
Figure 3.6	Protocol for minimizing background	26
Figure 4.1a	Calibration curves at 1atm and r(P) plots of C.SNAFL-1 and C.SNARF-1 in MOPS	29
Figure 4.1b	Calibration curves at 1atm and r(P) plots of C.SNAFL-1 and C.SNARF-1 in BES	30
Figure 4.2a	pH buffers’ pH(P) plots using C.SNAFL-1 and C.SNARF-1 in MOPS	31
Figure 4.2b	pH buffers’ pH(P) plots using C.SNAFL-1 and C.SNARF-5F in MOPS	32
Figure 4.3	Fluorescent spectra of DND-160 in acetate at different pHs.	34
Figure 4.4	Fluorescent spectra of DND-160 in high and low pH	35
Figure 4.5	Excitation wavelength dependence of the pKa	36
Figure 4.6	High pH Fluorescence emission at 1atm and 512 atm	37
Figure 4.7	Pressure induced shift of the high pH emission peak	37
Figure 4.8a	Calibration curves at 1atm and r(P) plots of DND-160	38

	in BES	
Figure 4.8b	Calibration curves at 1atm and r(P) plots of DND-160 in MOPS	39
Figure 4.9	Calibration curve at 1 atm and 510 atm of DND-160 in acetate, MOPS and BES.	40
Figure 4.10	Pressure dependency of high pH intensity ratios	40
Figure 4.11a	pKa(P) of DND-160 in acetate.	41
Figure 4.11b	pKa(P) of DND-160 in MOPS and BES	42
Figure 4.12	Single configuration coordinate model for intramolecular charge transfer	43
Figure 4.13	Scheme for pressure dependency of LE and CT states and there interaction	44

List of Abbreviations

DND-160	LysoSensor Yellow/Blue
C.SNAFL	seminaphthofluoresceins
C.SNARF	seminaphthorhodafluors
ICT	Intramolecular charge transfer
LE	Locally electronic
CT	Charge transfer
MOPS	3-(N-morpholino)propanesulfonic
BES	N,N-Bis(2-hydroxyethyl)-2-aminoethanesulfonic
BCECF	2',7'-bis-(2-carboxyethyl)-5-(and-6)-carboxyfluorescein
PRODAN	6-propionyl-2-dimethylaminonaphthalene
ADMA	p-(9-anthryl)-dimethylaniline
DPO	2,5-diphenyloxazole

Acknowledgements

I would like to thank my adviser, Dr. Paul Urayama, for his close guidance and great patience with me in doing this thesis, and for his willingness to help students achieve and for introducing me to the world of fluorescence and biophysics. Also, I would like to thank Dr. William Houk and Dr. Douglas Marcum for their inputs and help in the suggestion and evaluation of my thesis. To my labmates, Josh, Scott, Eric, Junaid and Dan, for their help and company in the lab. To Michael Eldrich, for helping me make the pressure chambers and chamber holders. To my classmates and to the physics department, for making my stay at Miami a memorable one. To my family and my wife, for all the support they gave me during this process.

CHAPTER I. INTRODUCTION

Pressure in the biosphere ranges from 0.1MPa to 110 MPa¹. Some microorganisms, which are called pieziophiles, thrive under extreme pressure conditions ¹. Varying pressure is also known to affect biological processes; these effects include cell adhesion ², morphology³, metabolism³, apoptosis³, growth¹ and protein folding⁴. Understanding the effects of changing the thermodynamic conditions, like pressure and temperature, are important in understanding the behavior and properties of living organisms. But compared to biological studies under temperature, pressure effects on biological systems are less investigated.

Pressurization causes the volume to decrease, causing a shift to a chemical reaction those results to a smaller volume. If we examine a chemical reaction of A and B, which then forms a product C, we get



and the equilibrium constant, K, of this chemical reaction is

$$K = \frac{[C]}{[A][B]}$$

During pressurization, the chemical equilibrium shifts to a system with lower volume. If C has a lower volume than the combined volume of A and B, K increases. Looking at the change of Gibbs free energy of the system, we have

$$\Delta G = \Delta U + P\Delta V - T\Delta S$$

where U is the internal energy, P is pressure, V is the volume, T is the temperature and S is the entropy. This change is due to the change of the Gibbs free energy before and after the chemical reaction of A and B. For a given chemical reaction in thermal equilibrium, the change of Gibbs free energy can be written as,

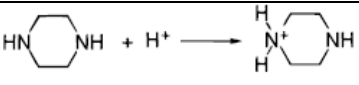
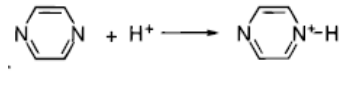
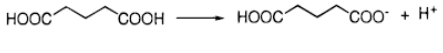
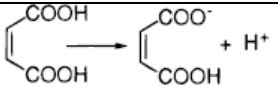
$$\Delta G = -RT \ln K ,$$

where R is the gas constant. During pressurization and if the temperature is held constant, the terms ΔU and $T\Delta S$ does not have any pressure dependence. Finally, we get the expression for the dependence of the equilibrium constant to pressure, the Arrhenius equation,

$$\frac{\partial(\ln K)}{\partial P} = -\frac{\Delta V}{RT} \quad 1.1$$

Equation 1.1 shows that pressure causes the equilibrium constant to shift to a state which has lower volume. Table 1.1 shows the ΔV of some ionic reactions.

Table 1.1. ΔV of some chemical reactions

Reaction	$\Delta V(\text{ml/mol})$	References
Dissociation of Water	-22.2	5
Dissociation of Acetic Acid	-11.2	5
Dissociation of Benzoic Acid	-11.7	5
	-5.6	6
	-6.3	6
	-23.0	6
	-5.5	6

One of the key biochemical parameters which has a significant effect on biological processes is pH. pH is important in cell homeostasis and cell behavior⁷⁻¹⁴. Living cells keep the pH within a certain range and large pH shifts inside or outside the cell's environment will interfere with some of its functions which can eventually cause diseases. In the mitochondria, a pH gradient between its inner and outer membrane is maintained for ATP generation; in some organelles, ATP is consumed to pump protons to it to maintain an acidic environment needed for processing and recycling of some proteins⁸. The ATP dependent proton pumps are called vacuolar H⁺-ATPases or V-ATPases⁸. The proton pumps work with proton leaks to regulate the pH in a cell. The pump and the leak model (*Figure 1.1*) says that the rate of proton pumping by the H⁺-ATPase is balanced by an equal out flow of protons through a H⁺ leak⁸. Some values of intercellular pHs are listed in *Table 1.2*.

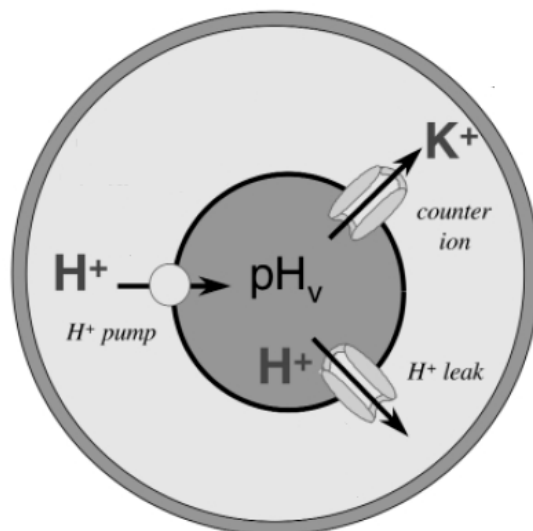


Figure 1.1. The “pump and the leak” model for maintaining intracellular pH⁸. Due to the electrogenic nature of both the H⁺ pump and leak, there functions can be limited by the permeability of the organelle to counterions(K⁺).

Table 1.2. List of some pH values of organelles/cells

Organelle/Cellular Fluid	pHs
Human Blood Cells	~7.26 ¹³
lysosome	<5.5 ⁸
Endosome	<6.0 ⁸
Golgi -apparatus	6.0-6.7 ⁸

Measurement methods for pH can be divided into these categories: pH test strips, electrode method, and indicator reagents¹². Commonly used pH strips are litmus paper which changes color in solutions with different acidity. A change in color is then compared to a standard to determine the pH of a certain liquid sample. The electrode method uses a electric probe which acts like a potentiometric sensor. It is composed of two electrodes, which measures the voltage. Indicator reagents are molecules whose spectroscopic properties change with pH. The changing spectroscopic property can be its absorbance or emission spectra. pH strips can be done the fastest but it can only be done in vitro, and it's the least accurate. The electrode is the most

common method in determining pH. Both the electrode and indicator method can be done in vivo and in vitro. The advantage of pH indicators compared to the electrode is that pH measurements done in vivo are much easier and it can be engineered to localize on a specific target, for example a lysosome.

Commonly used method using pH indicator reagents is pH fluorescence spectroscopy. Fluorescence pH probes have more advantages than absorption dyes. Fluorescent probes can be designed to have a longer and different emission wavelength, which can help minimize background interference. Absorbance usually happens on the UV or on the bluer side of the spectra which can also excite unwanted fluorophores. Fluorescence also has much better signal to noise since the intensity is measured directly from the dyes emission while absorbance entails measuring the light after being absorbed by the sample.

pH probe fluorescence depends on the emission properties of its protonated and deprotonated form. One or both chemical forms can be fluorescent. The concentrations of the chemical species determine the fluorescence of the probe. In a more acidic environment, the pH probe will prefer its protonated form. For a pH dye with a single dissociation, its chemical reaction is



and the equilibrium constant of this reaction is related to the pH by the Handerson-Hasselbalch equation

$$pH = pK_a + \log \frac{[D]}{[HD]} \quad 1.2$$

pH molecular probes have a working range of a couple of pH points (± 1.5) from its pKa. Probes with dual excitation or emission peaks can be used to measure pH ratiometrically. Ratiometric method are much more advantageous to use than absolute intensity probes, since there isn't a need to correct the intensity due to intensity loss caused by optical length, light scattering, illumination intensity and photobleaching¹⁵. The most common pH fluorescent probes are fluorescein, BCECF, SNAFLs, SNARFs¹⁶. The pKa's of these dyes are shown in table 1.3.

Table 1.3. List of some pH dyes [Invitrogen]

Dye	pKa	Measurement Wavelengths
fluorescein	~6.4	Excitation ratio 490 nm/ 450 nm Detected at 520 nm
BCECF	~7.0	Excitation ratio 490 nm/450nm Detected at 530 nm
C.SNAFL-1	7.8	Emission ratio 545 nm/ 620 nm Excited at 514 nm
C.SNARF-1	7.41	Emission ratio 580nm/640nm Excited at 514 nm

Intracellular pH measurements are routinely done under ambient pressure. Increasing pressure can cause a change in the pH of a cellular environment which can cause some physical effect on its behavior because large pH shift can affect cellular functions. For example, study done by Abe et. al, using 6-carboxyfluorescein diacetate, intracellular pH changed by 0.33 with pressurization up to 600 atm in *Saccharomyces Cerevisiae* yeast¹⁷. Fluorescent dyes were also used to measure the volume change (ΔV) of the acid-base reaction of pH buffers. Quinlan et. al. used C.SNAFL-1 to measure the ΔV of pH buffers¹⁸. Salerno, et al., calibrated pH fluorescent probes C.SNAFL-1, C.SNARF-1, C.SNARF-4F, and C.SNARF-5F for high pressure pH sensing. In this study, the ΔV of the fluorescent probe was measured and used to correct measured pH values from the fluorescence of the dye. Failure to incorporate this correction factor can make pH measurements inaccurate by 0.02 pH units for a change of pressure by 100 atm¹⁹.

Pressurization causes the change of the fluorescence of C.SNAFLs and C.SNARFs dyes due to the shift of its chemical equilibria¹⁹, since the emission and absorption spectra of these dyes are dependent on the concentration of its two chemical species, the protonated (low pH) and deprotonated (high pH) forms; and the fluorescence of these two forms were unchanged due to varying pressure. Also, the ΔV of the dissociation of the dye were buffer independent.

In this thesis, LysoSensor Yellow/Blue DND-160 is being investigated under high hydrostatic pressure. This dye is a low pH sensor and also a ratiometric dye like the C.SNARFs and

C.SNAFLs. The motivation for the development of this probe was due to the small number of low pH probes available at that time (1999) and also these were ill-adapted to study acidic organelles since their fluorescence was greatly reduced in acidic solutions²⁰. There was also a need of a low pH ratiometric probes since BCECF was the only one which was used in excitation ratiometric measurements. Aside from being a low pH probe, DND-160 also has a “push pull” electronic transfer system. This “push pull” mechanism is a intramolecular charge transfer (ICT) between the strong electron-donating group (alkoxy) and electron-withdrawing group (pyridinium)²⁰. Emissions of fluorophores with intramolecular charge transfer states are dependent on solvent polarity^{16,21}. Studies done by Rollinson and Drickamer on ICT molecules under pressure, PRODAN and ADMA, shows that there fluorescence properties changes under pressure^{22,23}.

Goals

The goals of this thesis are to investigate the change of fluorescence of LysoSensor Yellow/Blue (DND-160) under high hydrostatic pressure. The specific goals are to answer these questions:

- Can DND-160 be used as a low pH probe under high hydrostatic pressures?
- Given the different fluorescence mechanism of DND-160 compared to C.SNAFLs and C.SNARFs, what is the pressure dependence of DND-160 in different solutions?
- What is a possible mechanism for this pressure dependence?

CHAPTER II. FLUORESCENCE SPECTROSCOPY

Overview

This chapter discusses the theory of fluorescence. It is subdivided into three sections: fluorescence, dapoxyl dyes and pH sensing dyes. In the fluorescence section, the mechanism behind fluorescence is presented and how environmental conditions can affect its behavior is discussed. In the dapoxyl dyes (DND-160 is a dapoxyl-structured dye), it will talk about the properties of a chemical derived from 2,5-diphenyloxazole (DPO). In the last section, pH sensors and ratiometric pH sensing are described. The study of Salerno, et al ¹⁹ is also outlined, which describes fluorescence pH sensing under high hydrostatic pressures. The analysis of this thesis is based on that same paper.

Fluorescence

Fluorescence is a luminescence process in which a molecule absorbs light that makes it go to the excited state and then emits light when it goes back to a lower energy state. Molecules that fluoresce are called fluorophores. Fluorescence is due to transfer of the electron from a excited singlet state to a lower state, while phosphorescence, the other form of luminescence, is due to emission of the electron coming from a triplet excited state. Typical fluorescence lifetime is on the order of $10^8 \sim 10^9$ s, while phosphorescence lifetimes, ranges from milliseconds to seconds ¹⁶. The lifetime for phosphorescence is longer because the transition for an electron from a triplet excited state to a ground state is forbidden, which causes a slower transition rate.

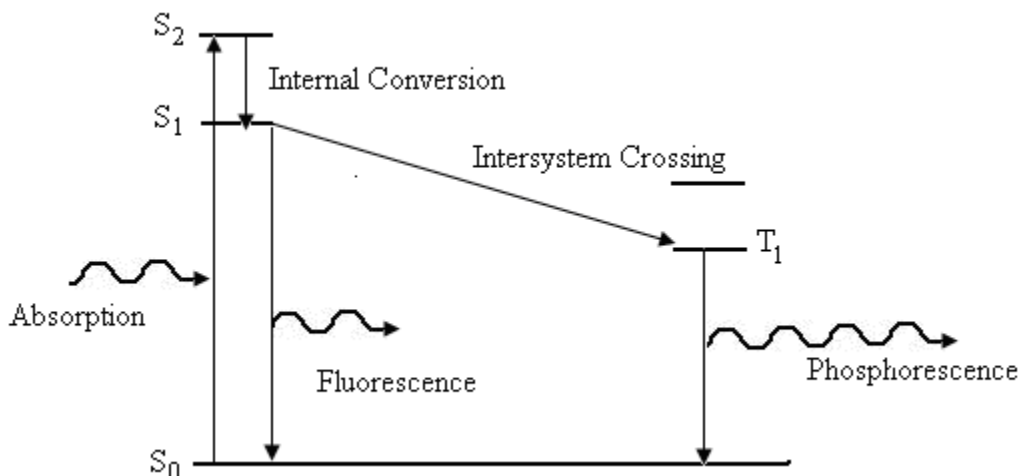


Figure 2.1. Simplified version of a Jablonski diagram. ¹⁶

The process of absorption and emission of light by molecules are best described using a Jablonski Diagram (*Figure 2.1*). When an incoming light is absorbed by a molecule, an electron from the ground state can be excited to some higher electronic state depending on the energy of the incoming light. In an electronic state, there are different possible vibrational states. An electron can relax to a lower electronic state or vibrational state; this is called an internal conversion. Due to internal conversion, fluorescence emission occurs when the electron goes back to the ground state. The emission wavelength is red shifted relative to the absorbed wavelength. This shift in the emission and absorption wavelength in fluorescence is known as the Stokes' shift (*Figure 2.2*). Phosphorescence happens when a photon is emitted when a S_1 molecule undergoes a spin conversion to a triplet state T_1 and then relaxes to its ground state. The transition from $S_1 \rightarrow T_1$ is called intersystem crossing. Transition from a singlet state to a triplet state is forbidden causing a slow reaction rate. The Jablonski diagram in *Figure 2.3* shows a simplified version that exclude interactions like quenching, solvent interactions and energy transfer. Quenching is a process in which the fluorescence intensity decreases ¹⁶. This can occur by various processes, one of which is by collision.

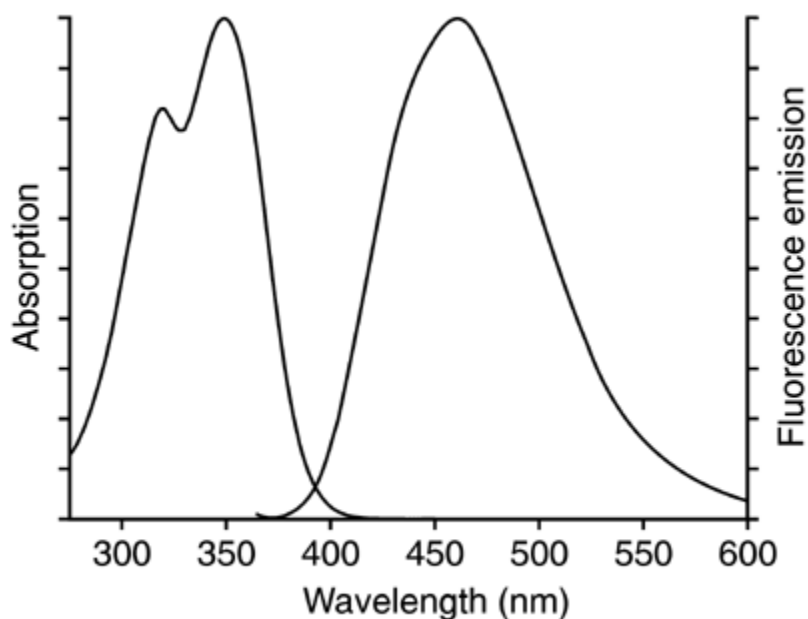


Figure 2.2. Absorption and emission spectra of quinine sulfate in water (Invitrogen)

The quantum yield of a fluorophore is the ratio of the number of photons emitted during fluorescence to the number of photons absorbed. The larger the quantum yield, the brighter the fluorescence. The quantum yield can be expressed as,

$$Q = \frac{\Gamma}{\Gamma + k_{nr}}, \quad 2.1$$

where Γ is the emissive rate of the fluorophore and k_{nr} is rate of the non-radiative decay¹⁶. The lifetime of the fluorophore is defined as the average time a fluorophore stays on an excited state before returning to a ground state. The lifetime can be expressed in terms of Γ and k_{nr} ,

$$\tau = \frac{1}{\Gamma + k_{nr}}. \quad 2.2$$

The value of the non-radiative decay, k_{nr} , is dependent on the interaction of the fluorophore with its environment. Some of this dependence is solvent interaction and fluorescence resonance energy transfer (FRET) (*Figure 2.3*). Fluorescence resonance energy transfer happens in which two molecules are used and their respective absorption and emission spectra overlap to one

another. The molecules that fluoresce are called the donor while the molecules which have absorption spectra that overlap with the donor's emission are called acceptors. The acceptor can also be a non-fluorescent molecule.

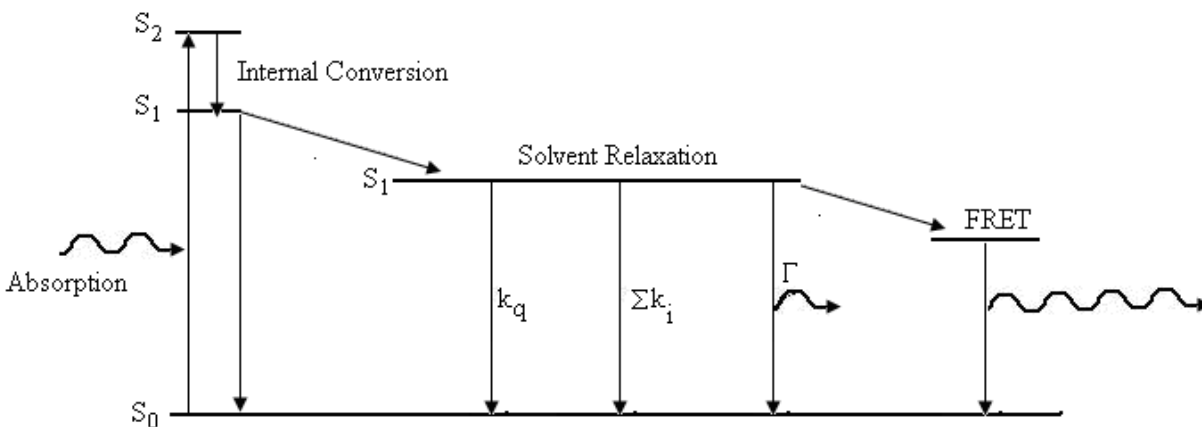


Figure 2.3. Jablonski diagram with FRET and quenching¹⁶. Σk_i are nonradiative processes which are not part of quenching and FRET.

Solvent Relaxation

Some of the factors that affect the dependence of the absorption and emission spectra of molecules are solvent polarity and viscosity, rate of solvent relaxation, changes of the fluorophore's conformation, internal charge transfer (ICT), proton transfer and excited state reactions, probe – probe interaction and changes in radiative and non-radiative decay rates¹⁶. Solvent polarity effects tend to shift the emission to a longer wavelength thus lower energy. A fluorophore usually has a larger dipole moment in the excited state (μ_E) than in the ground state (μ_G)¹⁶. Increasing the polarity of the solvent decreases the excited energy state of the fluorophore. Non-polar fluorophores are less sensitive to solvent polarity. The Lippert-Mataga equation gives the relationship of the dependence of the shift of the absorption and emission frequency to the polarity of the solvent. This theory neglects other interaction like formation of charge transfer state, hydrogen bonding and conformational changes. The Lippert-Mataga equation is,

$$\bar{\nu}_A - \bar{\nu}_F = \frac{2}{hc} \Delta f \frac{(\mu_E - \mu_G)^2}{a^3}, \quad 2.3$$

were $\Delta f = \left(\frac{\epsilon - 1}{2\epsilon + 1} - \frac{n^2 - 1}{2n^2 + 1} \right)$, ν_A and ν_E are the absorption and emission wavenumbers respectively, ϵ is the solvent's dielectric constant, n is the solvent's refractive index and a is the radius of the fluorophore's cavity. The dielectric constant and refractive index depends on the polarity of the solvent. The Jablonski diagram that includes solvent effects is shown in *Figure 2.4*.

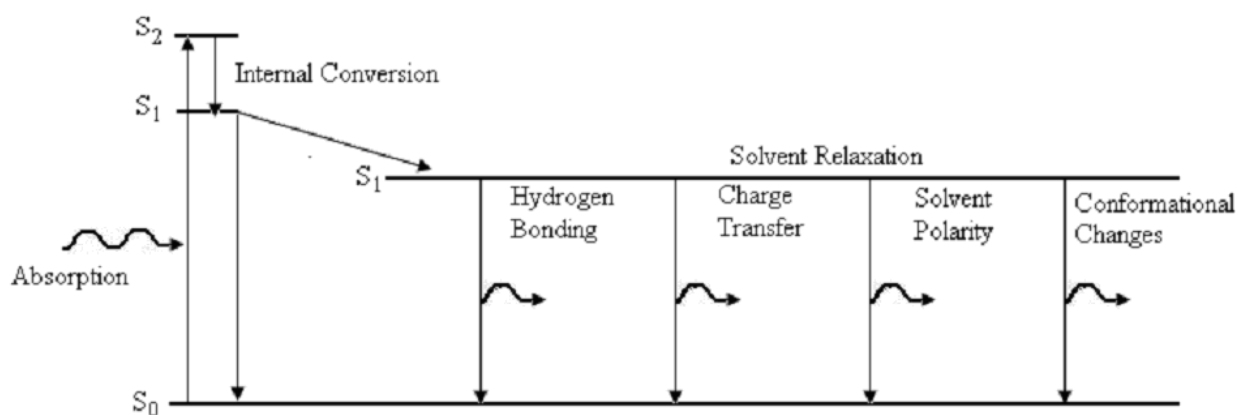


Figure 2.4. Jablonski diagram with specific environmental effects on the excited state

One way for the excited molecule to relax is by intermolecular charge transfer (ICT). Fluorophores that form an internal charge transfer state contain both an electron donating and acceptor group. Fluorescence can depend on the interaction between donor and acceptor groups. Fluorophores which have ICT states are also dependent on solvent polarity. For a polar fluorophore, the ICT state is lower than the locally excited (LE) state, but for a nonpolar fluorophore, it's the locally excited state which has higher energy¹⁶.

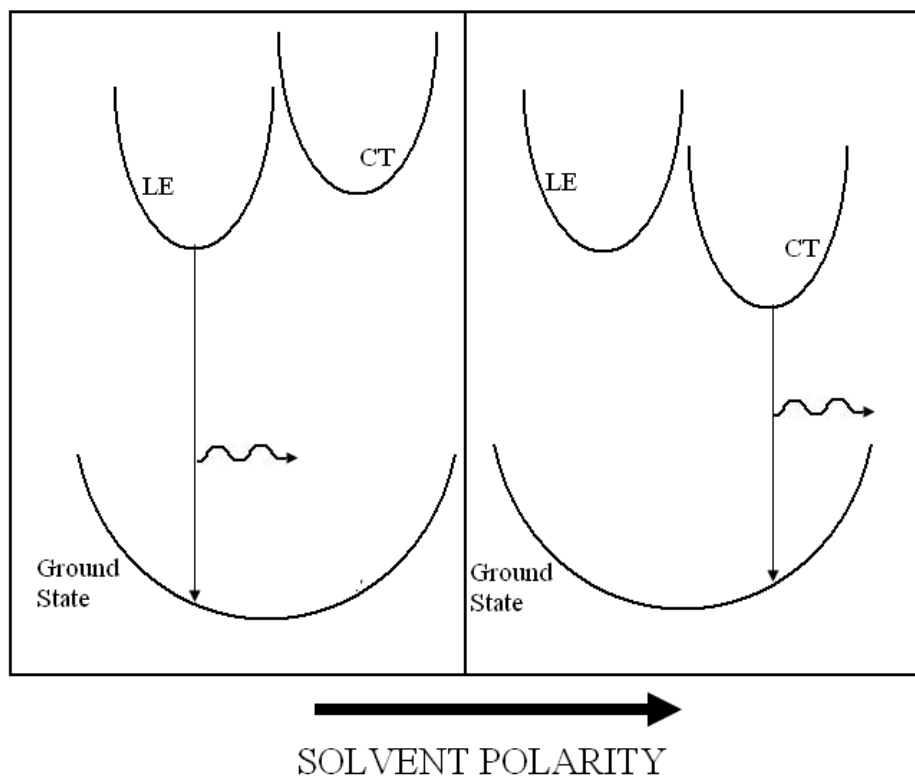


Figure 2.5. Solvent polarity dependence of a charge polar probe (left) charge transfer state

Dapoxyl dyes are a new set of probes that were developed as molecular probes that are highly sensitive to solvent polarity^{20, 21}. These types of fluorophore are more sensitive to solvent polarity than any other fluorophore^{16, 24}. Its structure is based on 2,5-diphenyloxazole (DPO). DPO has a high quantum yield but, by itself, does not have any solvent dependence. The dapoxyl dyes are formed by attaching an electron acceptor and donor groups to DPO. The structure and solvent dependence of a dapoxyl dye is shown in *Figure 2.6*

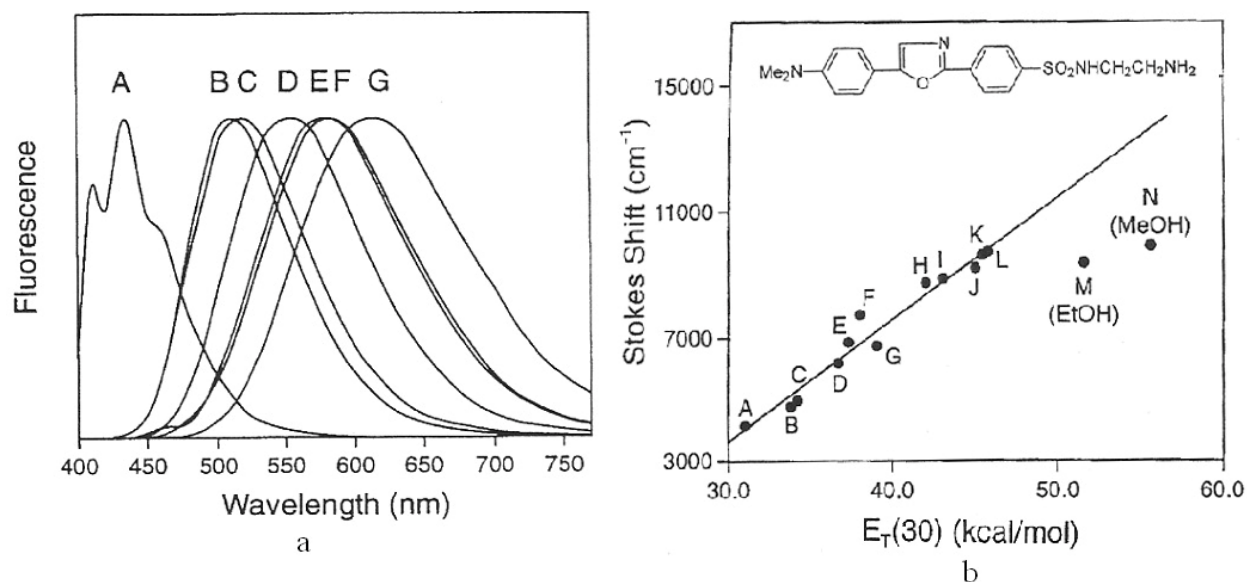


Figure 2.6. Emission spectra of Dapoxyl SEDA (dapoxyl sulfonyl ethylenediamine) in different solvents with increasing polarity (a). Stokes' shift dependence on solvent polarity (b). INSET : chemical structure of Dapoxyl SEDA ²¹ .

Fluorescence Measurements

Fluorescence measurements can be done by intensity, lifetime, and anisotropy measurements. Intensity measurements are done by absorption and emission modes. In absorption measurements, the absolute intensity of the fluorescence is measured at a given emission wavelength as the excitation wavelength is changed. In emission modes, the fluorescence is measured for a given excitation. In fluorescence lifetime, the rate of the decay of the fluorescence is being measured. This can be done by two modes: frequency and lifetime. In frequency mode, the fluorophore is excited by an oscillating light source, then the fluorescence response is also oscillating, the lifetime can be calculated from the phase shift of the fluorescence and the excitation. For the anisotropy measurements, the fluorophore is exposed to a polarized light source, only molecules that have their electric field vector aligned to the light source is excited. The magnitude of the fluorophores rotation during the excited state determines its polarization and anisotropy. Anisotropy measurements can give information about the size and shape of molecules and the rigidity of the environment ¹⁶ .

pH Sensing Dyes

Measurements of pH can be done using an electric probe, light absorbance measurements [10] or fluorescence measurements. In fluorescence spectroscopy, pH sensing dyes are used as pH probes. These probes can also be used to measure intracellular pH. The emission and absorption spectra of the dye is pH dependent. Carboxyfluorescein, BCECF, SNAFLs and SNARFs are some of the commonly used pH sensing dyes¹⁶. Emission of pH sensing dyes DND-160, C.SNAFL-1, C.SNARF-1 and C.SNARF-5F are shown in *Figure 2.7*.

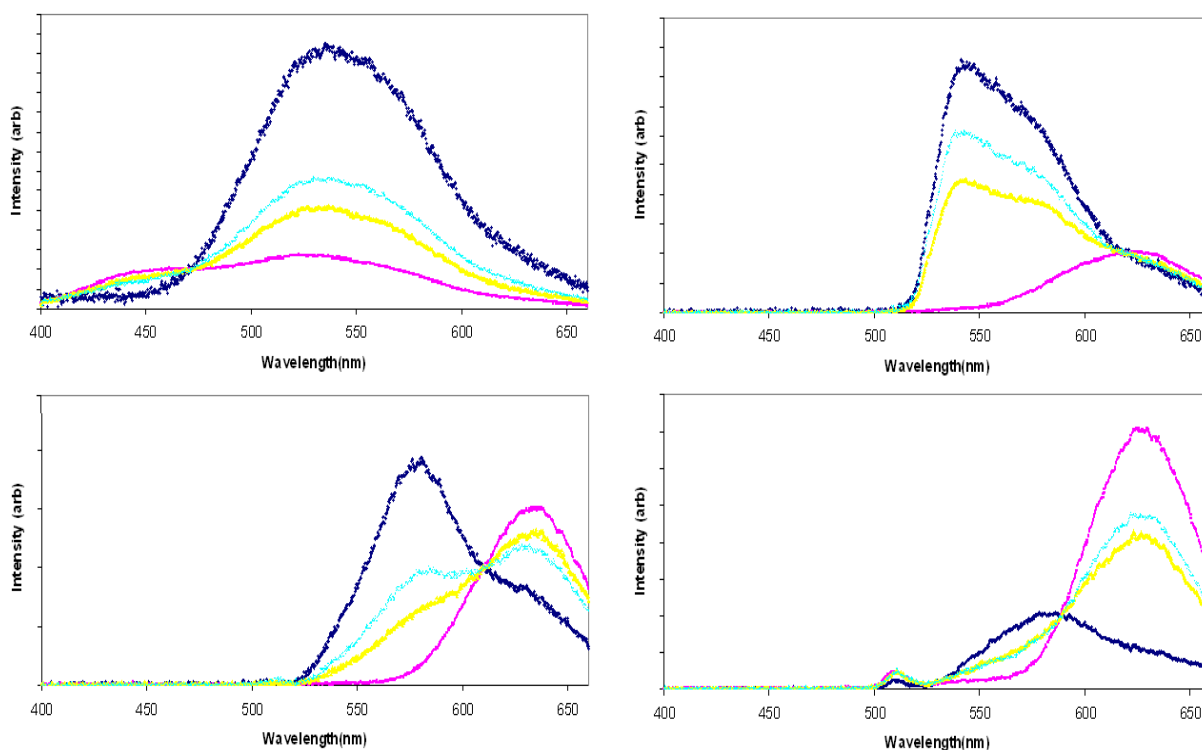


Figure 2.7. Fluorescence emission of pH sensing probes at different pH. Left to right from top row: DND-160, C.SNAFL-1, C.SNARF-1, and C.SNARF-5F. For the C.SNAFL-1 and C.SNARF dyes, the low pH spectra are shifted to the bluer peak while for DND-160's low pH spectra has a single peak at 540 nm. A 337 nm excitation source is used for DND-160 while a 500 nm dye laser is used for C.SNAFL and C.SNARF.

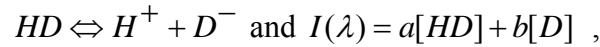
Two State Model

The fluorescence response of the pH sensing dye can be quantified by using a two-state model, where the fluorescence of the dye is due to the fluorescence of two chemical species, the protonated [HD] and the unprotonated [D] form. Since, a pH sensing dye is a weak acid, the concentration of its [HD] and [D] follows the Henderson-Hasselbalch equation,

$$pH = pK_a + \log \frac{[D]}{[HD]}.$$

When the dye is in a solution with a pH equal to its pKa, the concentration of its [HD] and [D] are equal. In a solution with pH >> pKa, the dye is mostly in its deprotonated form; in pH << pKa, it's mostly in its protonated form. The pKa of the dye determines the concentration of the protonated and deprotonated forms at a given pH.

If the two chemical species are fluorescent, the intensity at a given wavelength is a superposition of the two spectra. So,



where **a** and **b** are the intensities of [HD] and [D] at $I(\lambda)$ and [] denotes concentration. The intensity ratio becomes,

$$r = \frac{I_1}{I_2} = \frac{I(\lambda_1)}{I(\lambda_2)} = \frac{a_1[HD] + b_1[D]}{a_2[HD] + b_2[D]},$$

where **I₁** and **I₂** are the intensity at λ_1 and λ_2 . Extracting the value of [D]/[HD] from the above equation. We have

$$r = \frac{a_1 + b_1 \frac{[D]}{[HD]}}{a_2 + b_2 \frac{[D]}{[HD]}} \Rightarrow r \left(a_2 + b_2 \frac{[D]}{[HD]} \right) = a_1 + b_1 \frac{[D]}{[HD]},$$

$$\frac{[D]}{[HD]} = \frac{b_1 - rb_2}{ra_2 - a_1} = \frac{\left(\frac{b_1}{b_2}\right)^{-r}}{r - \left(\frac{a_1}{a_2}\right)} \times \left(\frac{b_2}{b_1}\right).$$

The value of r at low pH depends only on $a_1[HD]/a_2[HD]$ because $[HD] \gg [D]$. Also r at high pH is $b_1[D]/b_2[D]$. Using the Henderson-Hasselbalch equation,

$$pH = pK_a + \log \frac{[D]}{[HD]},$$

we get,

$$pK_a = pH + \log \left[\frac{r - r_{highpH}}{r_{lowpH} - r} \times G \right], \quad 2.4$$

r_{highpH} and r_{lowpH} are the ratio at low and high pHs. G is the ratio of b_2/a_2 . b_2 can be measured by getting the value of I_2 at high pH and scaling it from the isosbestic point. The isosbestic point is the wavelength in which the emission intensity is similar for the two chemical species ($[H]$ and $[HD]$). This also means that the intensity at the isosbestic point for a pH dye is the same at different pHs. The value of a_2 can be determined by the same procedure but at low pH. The value of G becomes 1 if I_2 is the isosbestic point. Using *Equation 2.4* to fit a fluorescence intensity ratio calibration curve, we can determine the pKa of the dye.

Fluorescence pH Sensing under High Pressure¹⁹

Fluorescence of pH sensors depend on the equilibrium of its protonated and deprotonated form. This equilibrium constant is pressure dependent. The pressure dependence of the equilibrium constant, K_a , can be seen in the Arrhenius relation (*Equation 1.1*). Applying this pressure dependence to *Equation 2.4*, we have,

$$pK_a(P) = pH(P) + \log \left[\frac{r - r_{highpH}}{r_{lowpH} - r} \times G \right],$$

where $pK_a(P)$ is the pressure dependent pKa of the dye, and $pH(P)$ is the pH change of the solution due to pressure. The pH of the solution is determined by the pH of the buffer solution

since the concentration of the dye is small compared to the buffer (2 μ M vs. 50 mM). The pH(P) of the buffer is,

$$pH(P) = pH(P_0) + \frac{1}{\ln 10} \frac{(P - P_0) \Delta V_{buffer}}{RT}, \quad 2.5$$

where ΔV is the volume change of the buffer dissociation and pH(P_0) is the measured pH of the buffer (1 atm in this thesis). The pressure dependent pKa of the dye can also be written as,

$$pK_a(P) = pK_a(P_0) + \frac{1}{\ln 10} \frac{(P - P_0) \Delta V_{dye}}{RT} \quad 2.6$$

CHAPTER III. INSTRUMENTATION AND METHODS

Overview

This chapter describes the experimental set-up and the materials used in this thesis. It is subdivided into three sections: sample preparation, instrumentation and data analysis. In sample preparation, it discusses what dyes and buffers were used and their preparation; in the instrumentation section, it shows the instruments used to excite and gather spectral data from the sample, and how the sample was pressurized; in the analysis section, it shows how the spectra were gathered and analyzed. Also, in the last section, the background spectrum is discussed and the importance of minimizing it.

Sample Preparation

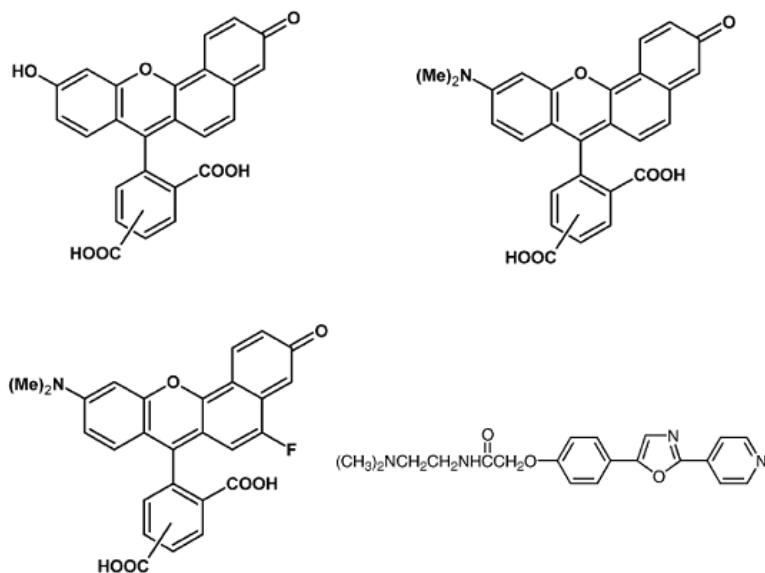


Figure 3.1. Chemical structures, left to right from top row: C.SNAFL-1, C.SNARF-1, C.SNARF-5F and DND-160. Protonation site for C.SNAFLs and C.SNARFs is 3-position oxygen while for DND-160 is the pyridyl group.

The pH sensing dyes and buffers were made by using 18.2 M Ω .cm deionized water (USFilter Purelab Ultra Polisher). The chemical structures of the pH dyes and buffers are shown in *Figure 3.1*. The dyes chosen in this thesis were LysoSensor Yellow/Blue DND160 (2-(4-pyridyl)-5-((4-

(2-dimethylaminoethyl-aminocarbonyl)methoxy) phenyl) oxazole, C.SNAFL-1(3,10-dihydroxy-3'-oxy-spiro[7H- benzo [c] xanthene -7- yl]-benzenedicarboxylic acid, C.SNARF-1 (2(or 4)-[10-(dimethylamino)-3-oxo-3H-benzo[c] xanthene-7-yl]- benzene dicarboxylic acid), and C.SNARF-5F(CAS name unavailable). The C.SNARF and C.SNAFL dyes were selected for this thesis because they have literature values for their ΔV and these dyes can be used to characterize pH buffers under high hydrostatic pressures. The dyes were purchased from Molecular Probes. C.SNAFL and C.SNARF dyes were in a free acid form while DND-160 was in DMSO. 20 μM stock dye solutions were made and stored at 4°C. The buffers used were acetate (pKa=4.8), 3-(N-morpholino)propanesulfonic/MOPS (pKa= 7.2), and N,N-Bis(2-hydroxyethyl)-2-aminoethanesulfonic/BES (pKa = 7.1). These buffers were selected for this thesis because DND-160 was to be investigated under pressure in two different solutions; acetate is a low pH buffer, while BES and MOPS are near neutral pH buffer. The buffers were purchased from Sigma-Aldrich. pH buffers, BES and MOPS, were made from free acid forms, while acetate were made from sodium acetate. Buffer stock solutions of 0.5 M were made and these were used to make another set of 0.055 M buffer stock solutions at a certain pH. The titration of the buffers was done using HCl and NaOH. For the MOPS and acetate buffers, two sets of pH solutions were made (for pH buffer pressure calibration and DND-160 calibration). For each set at least five pH solutions were made; two pH solutions were at extreme pHs ($\text{pH} \gg \text{pKa}$ and $\text{pH} \ll \text{pKa}$) and at least three at intermediate pHs ($\text{pH} \approx \text{pKa}$). These buffer stock solutions were stored at room temperature (294K). The pHs of the buffers were measured at 1 atm using a three point calibration pH meter. Calibration was done using three buffer standards (pH 4.00, pH 7.00 and pH 10.00 purchased from Fisher Scientific). The pH meter has an accuracy of 0.02 pH units. The pH of the buffer was checked before mixing it with the dye. The final sample has a concentration of 2 μM dye in a 50mM buffer solution.

Instrumentation

Spectral data was collected using a custom built high-pressure spectrofluorimeter system as shown in *Figure 3.2*^{25, 26}. The excitation source was a pulsed nitrogen laser (337 nm, GL-3300 Photon Technology International). The laser output was focused to a custom-built high pressure microscopy chamber. The design of the high pressure microscopy chamber was done by Raber,

et, al, 2006²⁷. The quartz capillary used for the chamber has an outer diameter of 1.5 mm and an inner diameter of 0.5 mm. For the UV excitation set up (I), a converging lens coupled with a controlled aperture focused the fluorescence of the sample into a fiber optic path to an inline filter which was used to hold a 385 nm high pass filter. The inline filter was then connected to a spectrograph (MS125, Oriel Instruments) and ICCD (iStar DH734, Andor Technology) using an optical fiber. The spectrograph has a resolution of 2 nm. For the green excitation set-up (II), tuning the dye laser to 500nm, a converging lens was used to focus the beam to an optical path to an inverted microscope (Zeiss). The output of the microscope was then filtered using a 485 nm long pass filter. A converging lens then focused the beam to an optical path to the spectrograph and ICCD.

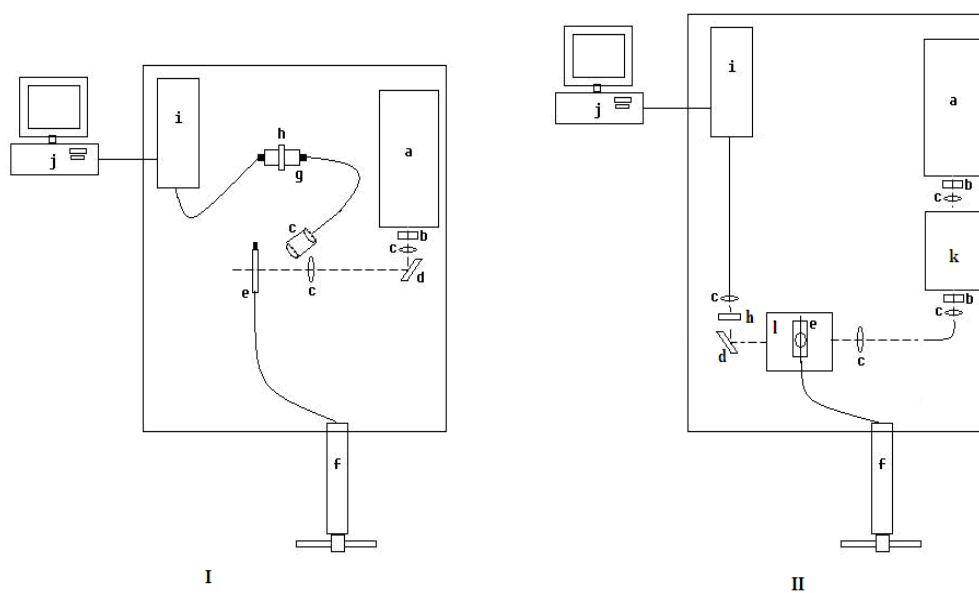


Figure 3.2. Schematic diagram of the experimental setup for UV excitation (I) and 500nm excitation (II): ^anitrogen laser, ^bneutral density filter, ^cconverging lens, ^dmirror, ^ehigh pressure microscopy chamber, ^fpressure generator, ^ginline filter, ^hlow pass filter, ⁱspectrograph and ICCD, ^jcomputer control, ^kdye laser, ^linverted microscope, ---- laser beam path

The pressure inside the chamber was controlled by a manual mechanical pump (37630, High Pressure Equipment) using a 50/50 ethanol-water mixture; the pressure of the chamber was measured using a Bourdon strain gauge (6PG30, High Pressure Equipment). The uncertainty of the reading of the pressure gauge was $\pm 3\%$. After each pressure change, the chamber was allowed to equilibrate for at least 10 minutes. There were at least seven pressure points where the spectra were recorded. The pressure of the chamber can go up to 600 atm. When decreasing the pressure, spectra on two pressure points (1 atm and 306 atm) were checked. This was done to check for any change of the spectra of increasing and decreasing pressure. In this thesis, there were no changes of the spectra when it was checked as the pressure was lowered.

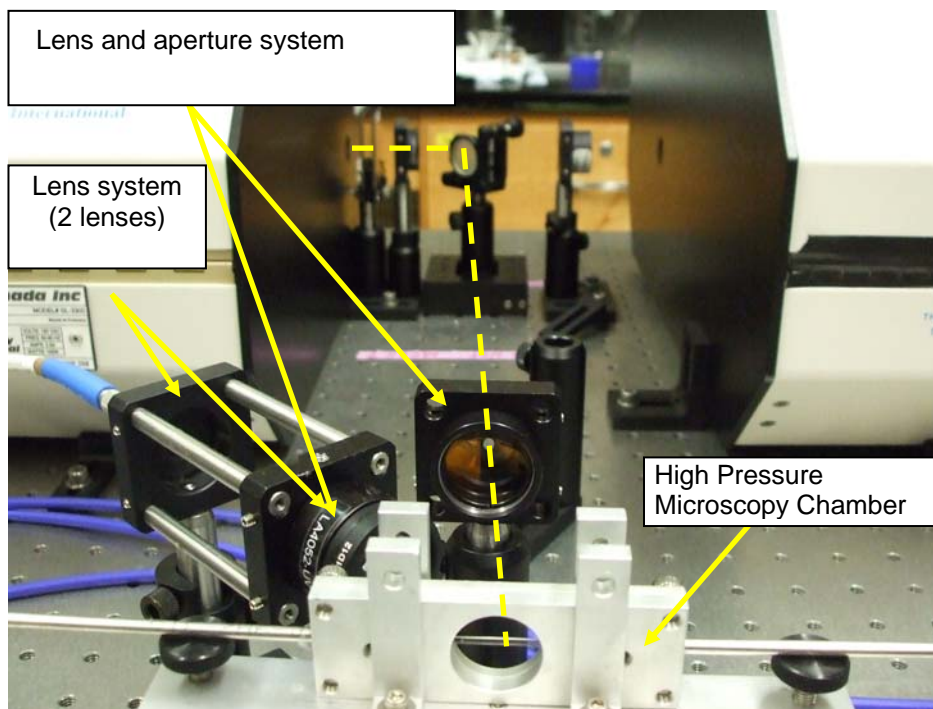


Figure 3.3 High pressure chamber and lens system. The incoming laser UV beam (dashed line) was guided to a lens and aperture system which controls and focus the beam going to the capillary.

Data Collection

The emission spectral data were collected using the IStar Andor software. The data were collected by getting the average of 15 to 30 individual spectra to improve signal to noise. The gain of the ICCD was set to 100-150 to increase signal intensity. Also, the ICCD gate width was set to 60 μ s to reject unwanted light. The intensity ratios measured were gathered from 10 spectral data sets. The standard deviation of the intensity ratios were a measure of dispersion from 10 values. The intensity ratios were calculated using the intensity at two wavelengths of the ratiometric dyes: C.SNAFL-1, C.SNARF-1, C.SNARF-5F and DND-160. The intensities were measured at a certain wavelength by using a 10 nm window on the measured spectrum (example for DND-160 in *Figure 3.4*). For this thesis, the ratios chosen for the dyes except C.SNARF5F were one of the emission peaks and the isosbestic point of the fluorescent dye (see *Table 2*).

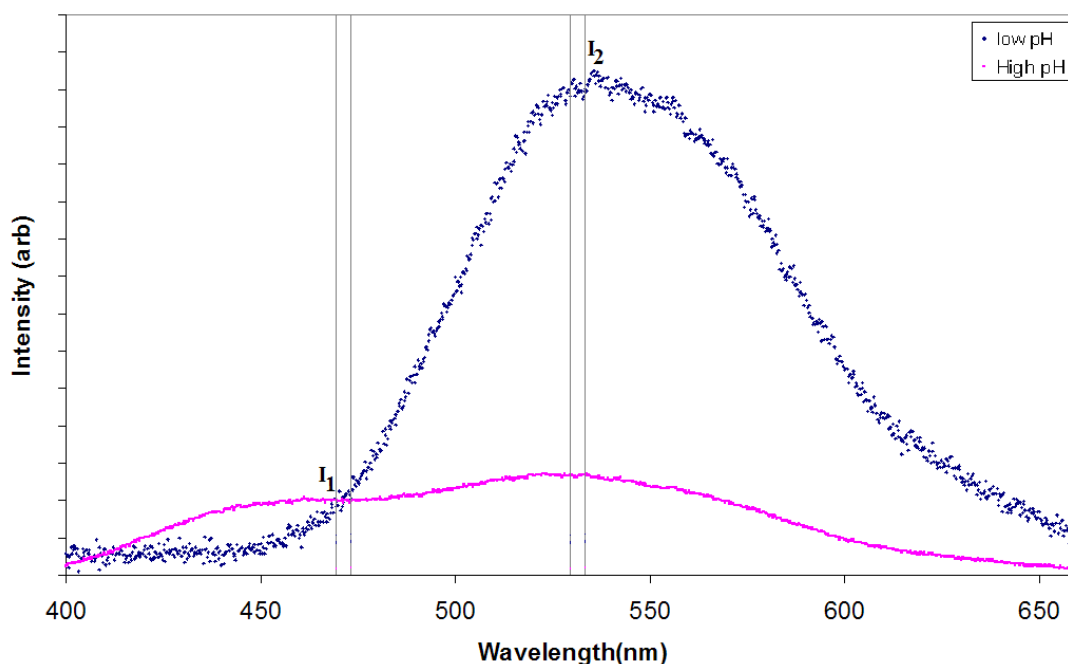


Figure 3.4. Fluorescence of DND-160 in its low and high pH form. The broad dark lines show the choice of two intensity wavelength to calculate the intensity ratio.

Table 3.2. Intensity wavelength window

Dye	Intensity wavelength windows		Isosbestic point
C.SNAFL-1	637 nm	610 nm	610 nm ⁷
C.SNARF-1	545 nm	620 nm	620 nm ⁷
C.SNARF-5F	625 nm	568 nm	588 nm ⁷
DND-160	523 nm	470 nm	470 nm

The background spectra of the high pressure microscopy chamber were routinely checked before and after each pressure run. When the chamber was exposed to a 500 nm light source, no background emission was detected but when it was UV excited, background emission was detected. The background spectra using the pressure chamber with deionized water has a peak between 410 nm to 450 nm as shown in *Figure 3.5*. In a fixed lens system, the background spectrum did not change when deionized water or an acetate buffer solution was flushed into the high pressure chamber but it changes when the lens system was changed.

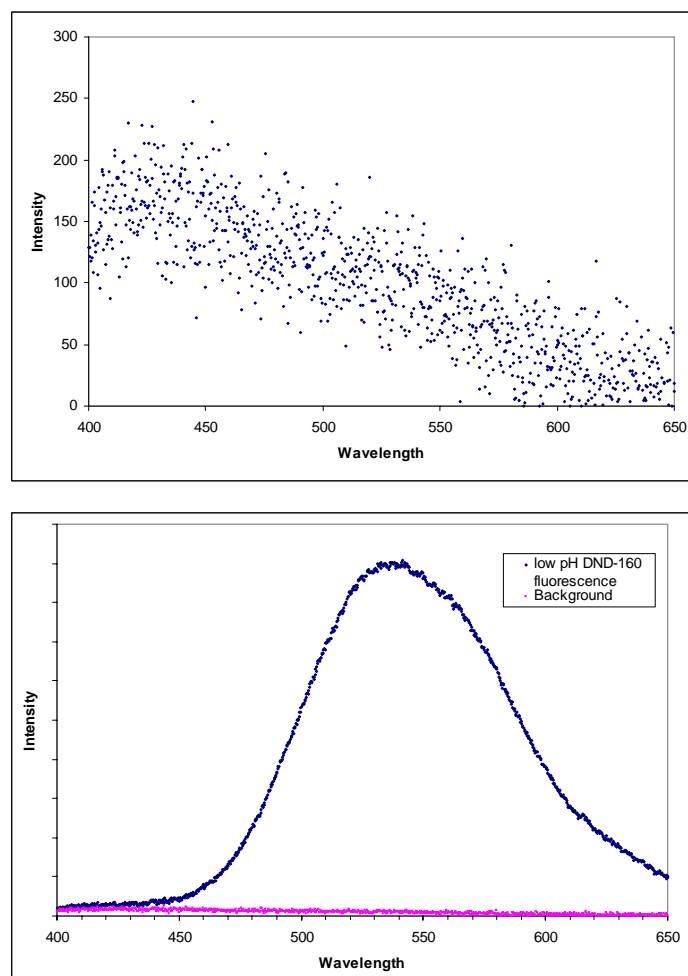


Figure 3.5. Background spectrum and low pH fluorescence of DND-160 in MOPS. Top to bottom: Background of the capillary chamber in deionized water; Background spectra with fluorescence emission.

One major obstacle in this thesis was the background emission when using UV excitation. The background fluorescence peak varies from 410 nm to 450 nm depending on the strength of the excitation and positioning of the lens. If the wavelengths of the isosbestic point and the low pH emission peak of DND-160 was 50 nm longer this effect would be negligible. With uncorrected background, the error in the measured intensity ratios increased and hysteresis of intensity ratios with pressure was observed. So there was a need to minimize the background and setup a quantitative value of minimizing it. The value was that the intensity ratio should not vary by 5% from the intensity ratio of the low pH form of DND-160 at 1 atm using a fresh capillary. The 5% criteria were selected because the intensity ratio measured using fresh capillaries did not vary by

5% from the average value. Background spectra were not detected using new capillaries, so this suggested that the background can be caused by the epoxy that was used to make the high pressure chamber or it could be something that was stuck in the chamber that fluoresce. The low pH intensity ratio was greatly affected by the background emission since it has a low intensity at 470 nm. At low pH, the intensity ratio was approximately at 6, so

$$r \approx 6 \approx \frac{I_2}{I_1}$$

If the criterion was 5% from the correct r , the range for the accepted r was 5.7-6.3. With the intensity ratio at the lower limit,

$$5.7 \approx \frac{I_2}{I_1 + \Delta},$$

where Δ was the intensity difference at wavelength 470 nm and 525 nm of the background. Solving for Δ ,

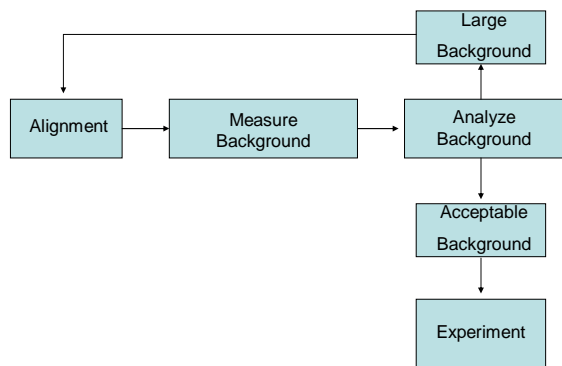
$$\Delta \approx 0.009I_2, \text{ for the higher limit, } 6.3, \Delta \approx -0.008I_2.$$

For $\Delta = -0.008I_2$, this means that the background intensity at 525 nm was greater than 470 nm. If the intensity of the low pH form at 525 nm was 10000 counts, the limit of Δ should be 80.

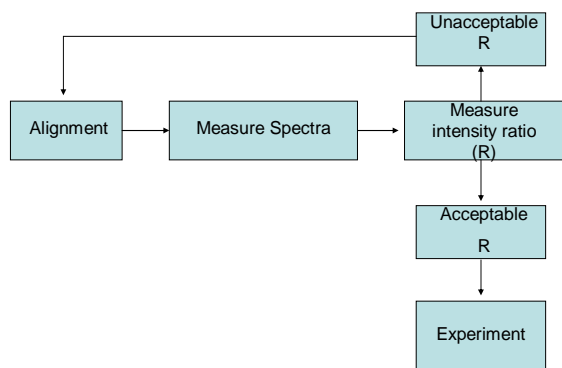
The spectra can also be corrected by looking at the intensity ratio of the dye. If the dye's intensity ratio varies a lot (more than %5 from the average value) compared to the capillary values, it signifies that the background was affecting the spectra of the dye. Otherwise, if r has the correct value, the background has been minimized.

The intensity of the background spectra was minimized using the lens system. This procedure was done by: increasing the neutral density to decrease the power of the incoming beam, changing the size of the aperture, and aligning the lens system. This method can also diminish the fluorescence intensity of the dye sample.

Minimizing the background was necessary for an experiment to proceed. Failure to do this correction can affect the observed spectra, consequently affecting the intensity ratio then the analysis of the results. This procedure was tedious; the lens system used for acquiring spectra has to be aligned at a point where the excitation beam has been focused. The summary for the protocol regarding the background is shown in *Figure 3.6*.



a



b

Figure 3.6. Protocol of minimizing background. (a) Using the 5% criteria for background. The background is measured first and alignment is done to minimize background. (b) Emission intensity is measured then r was calculated. The experiment proceeds based on the error of the intensity ratio.

CHAPTER IV. RESULTS AND DISCUSSIONS

Overview

This chapter talks about the results of the buffer and DND-160 characterization under high hydrostatic pressures. For the buffer characterization, the value of the ΔV of MOPS and BES were obtained using pH sensing dyes C.SNAFL-1 and C.SNARFs. In the DND-160 section, the fluorescence of DND-160 in acetate, BES and MOPS under high pressures were shown. The ΔV of the dye was also determined and its value shows some solvent dependence. In the discussion section, it talks about possible mechanisms for the fluorescence of DND-160 and its response under pressure.

Buffer Characterization

The emission spectra of a pH dye are dependent on the concentration of its protonated and deprotonated forms. Also, the concentration of these two chemical species is dependent on the pH of the solution and also the equilibrium constant of the dye. Since, the pH of the solution (which is set by the pH of the buffer) and the equilibrium of the acid-base reaction of the dye are pressure sensitive, the pressure response of the fluorescence of the dye is an apparent effect caused by the change of the pH of the solution and also the change of the chemical equilibria of the dye. In order to quantify the pressure effect of a pH sensing dye, the buffer used must first be characterized under pressure. In this thesis, characterization of a pH buffer or a pH dye under pressure means that the ΔV , which is the volume change of the acid dissociation of the buffer or dye, is determined.

In this thesis, the ΔV of buffers BES and MOPS were measured using fluorescent pH sensing dyes seminaphthorhodafluors (SNARF's) and seminaphthofluoresceins(SNAFL's). The C.SNAFLs and C.SNARFs dyes were selected in this study because the known value of its ΔV ¹⁹. The ΔV and pKa of the dyes are shown in *Table 4.1*. The technique for measuring the ΔV_{buffer} is the same as describe by Salerno, et al¹⁹ (see *Chapter 2*).

Table 4.1. pKa and ΔV of C.SNAFL and C.SNARF dyes¹⁹

Dye	Literature pKa	ΔV_{dye} (ml/mol)
C.SNAFL-1	7.76	-8.2
C.SNARF-1	7.41	-7.6
C.SNARF-5F	7.37	-8.0

The calibration curve and pressure dependence of the intensity ratios of the fluorescent dyes used are shown in *Figure 4.1*. The intensity ratios (r) at intermediate pHs changes linearly with increasing pressure while r_{highpH} and r_{lowpH} does not have any pressure dependence. This behavior is in good agreement with the literature result¹⁹. Using the r_{highpH} , r_{lowpH} , G , $pK_{a\text{dye}}$ on *Equation 2.4*,

$$pK_a(P) = pH(P) + \log \left[\frac{r - r_{\text{highpH}}}{r_{\text{lowpH}} - r} \times G \right] \quad 2.4$$

and rearranging Equation 2.4,

$$pH(P) = pK_a(P) - \log \left[\frac{r - r_{\text{highpH}}}{r_{\text{lowpH}} - r} \times G \right]$$

the value of the pH at a particular pressure can be determined. When only using the pKa of the dye at 1atm, the pH(P) is the apparent pH change effect under pressure due to the change of the chemical equilibria of both the pH buffers and the dye. In order to get the corrected pH(P), the correction for the pKa(P) is needed. Using ΔV_{dye} and *Equation 2.6*,

$$pK_a(P) = pK_a(P_0) + \frac{1}{\ln 10} \frac{(P - P_0) \Delta V_{\text{dye}}}{RT} \quad 2.6$$

the effect of pressure to the dye's pKa is determined. The corrected pH(P) plots are shown in *Figure 4.2*.

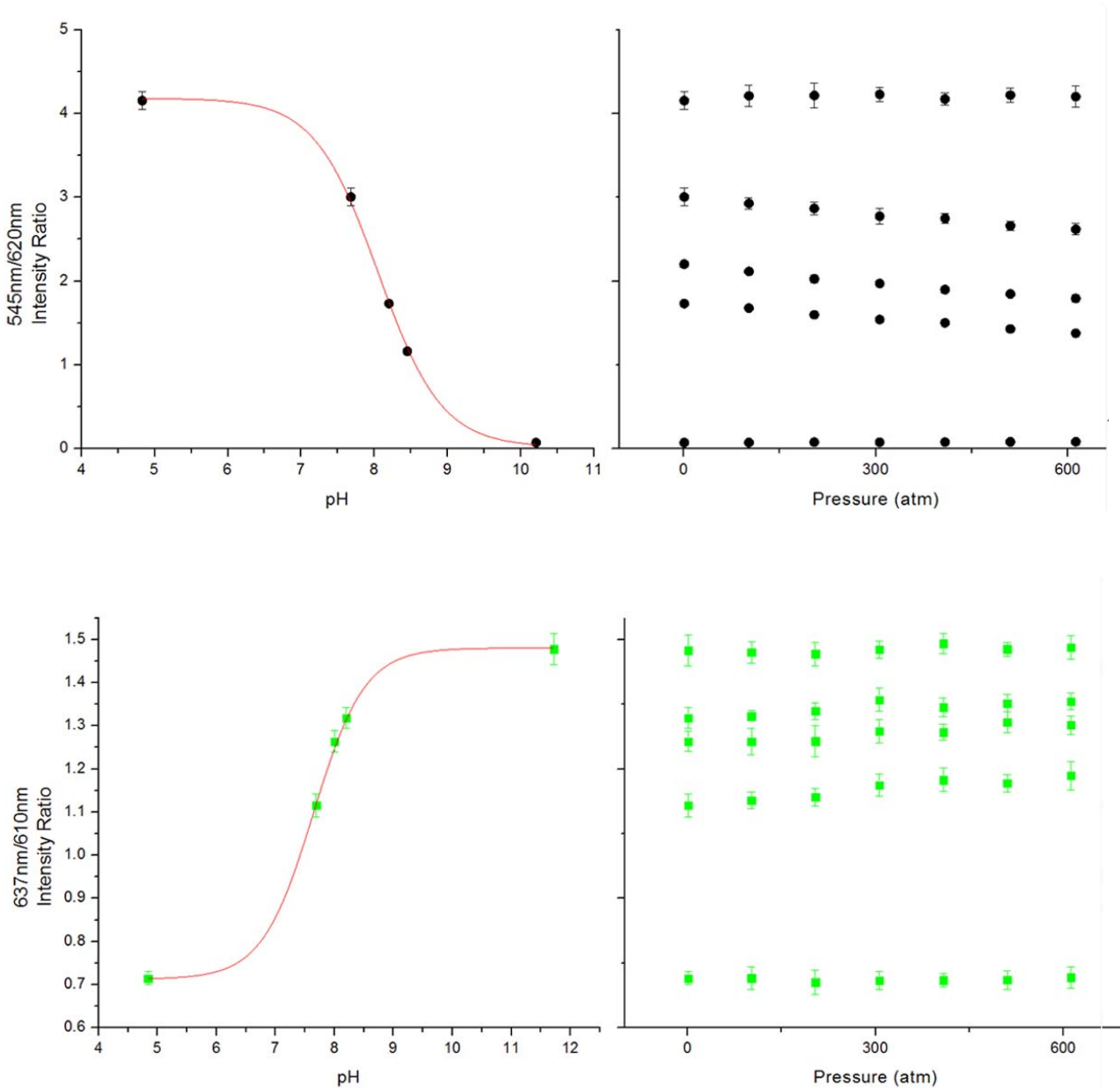


Figure 4.1.a. Calibration curves at 1 atm and r(P) plots of C.SNAFL-1(top) and C.SNARF-1 of MOPS. The data in the calibration curve(left side) are the measured intensity ratios at different pHs. The line in the calibration curve is a fit using *Equation 2.4*. The error bars are the standard deviation of 10 measurements.

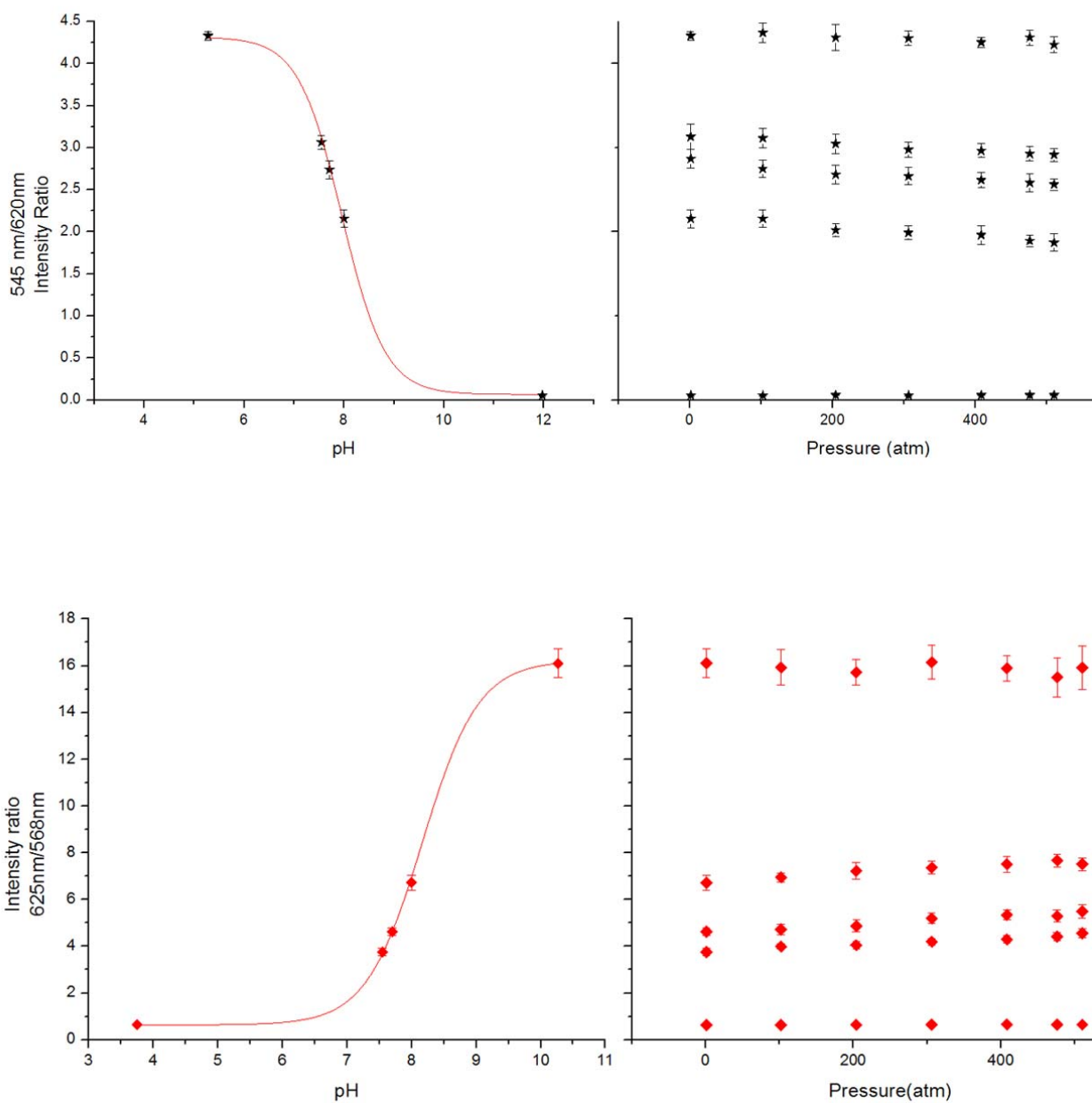


Figure 4.1.b Calibration curves at 1 atm and $r(P)$ plots of C.SNAFL-1 and C.SNARF-5F in BES

The line in the calibration curve is a fit using *Equation 2.4*. The error bars are the standard deviation of 10 measurements.

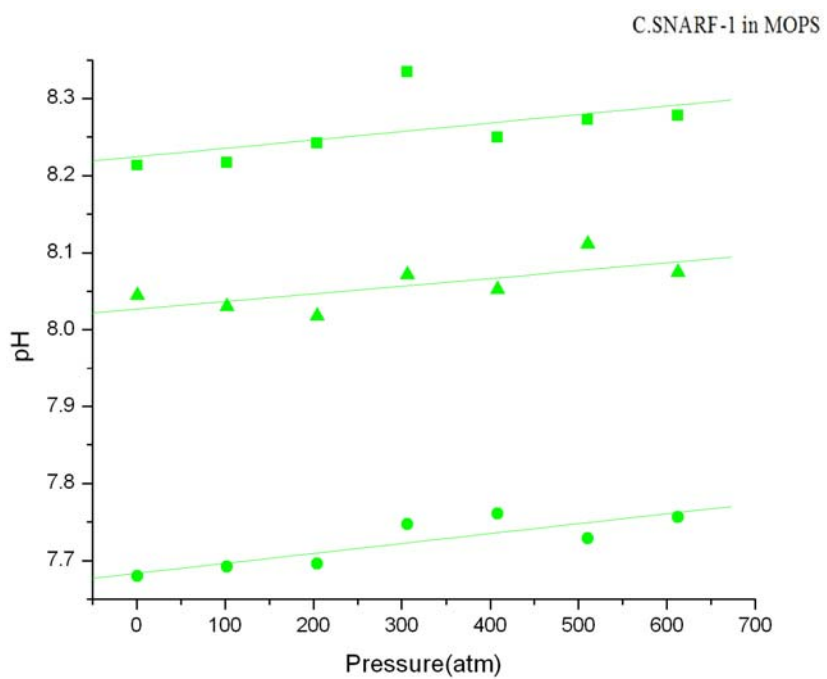
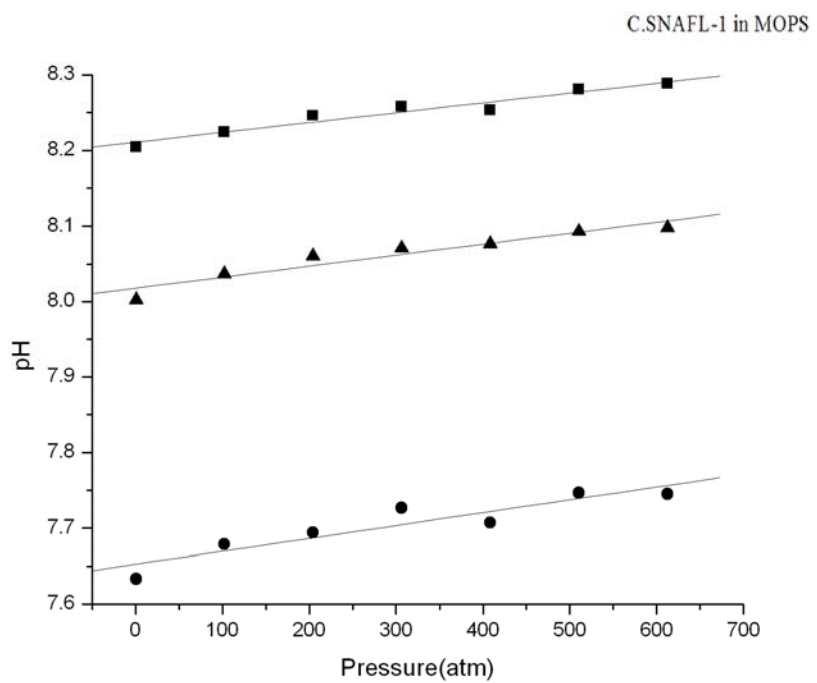


Figure 4.2.a. pH buffers' pH(P) plots using C.SNAFL-1 and C.SNARFs in MOPS

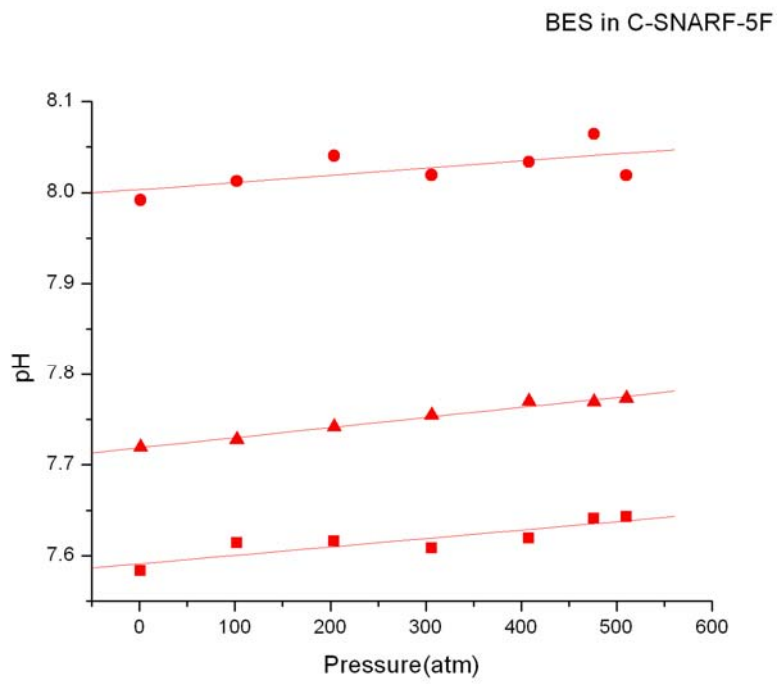
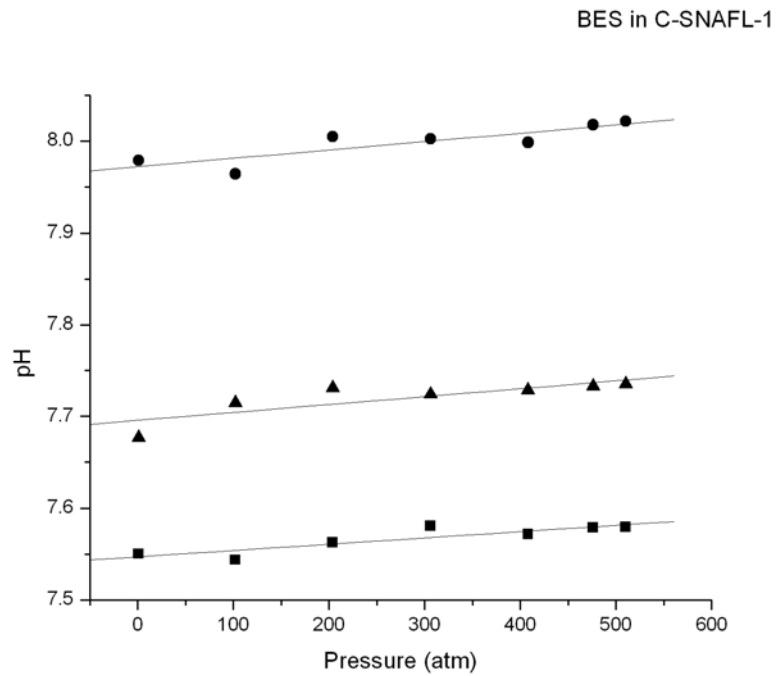


Figure 4.2.b. pH buffers' pH(P) plots using C.SNAFL-1 and C.SNARFs in BES

Figure 4.2 shows the corrected pH measurements under pressure using C.SNAFL and C.SNARF. These corrected plots were done after incorporating the pressure dependent pKa of the dye. The ΔV_{buffer} values can be obtained from the slope of the pH(P) using Equation 2.5,

$$pH(P) = pH(P_0) + \frac{1}{\ln 10} \frac{(P - P_0) \Delta V_{\text{buffer}}}{RT} . \quad 2.5$$

The values of ΔV_{buffer} using two pH probes and the literature value of the ΔV of acetate are shown in Table 4.2.

Table 4.2. ΔV of pH buffers

Buffers	$\Delta V_{\text{buffer}}(\text{ml/mol})$ / Dye used		Average $\Delta V_{\text{buffer}}(\text{ml/mol})$
MOPS	7.67 ± 0.62 /C.SNAFL-1	6.45 ± 0.63 /C.SNARF-1	7.06 ± 0.86
BES	4.54 ± 0.65 /C.SNAFL-1	4.21 ± 1.10 /C.SNARF-5F	4.37 ± 0.24
Acetate			-11.2^5

DND-160 results

The goal of this thesis is to investigate the pressure effects of the fluorescence of DND-160. The pressure effect of the fluorescence of DND-160 is an effect due to the pressure induced change of the dye and also the solution used. After determining the ΔV_{buffer} of MOPS and BES, we can quantify the pressure effect of DND-160 in these solutions.

Fluorescence Emission

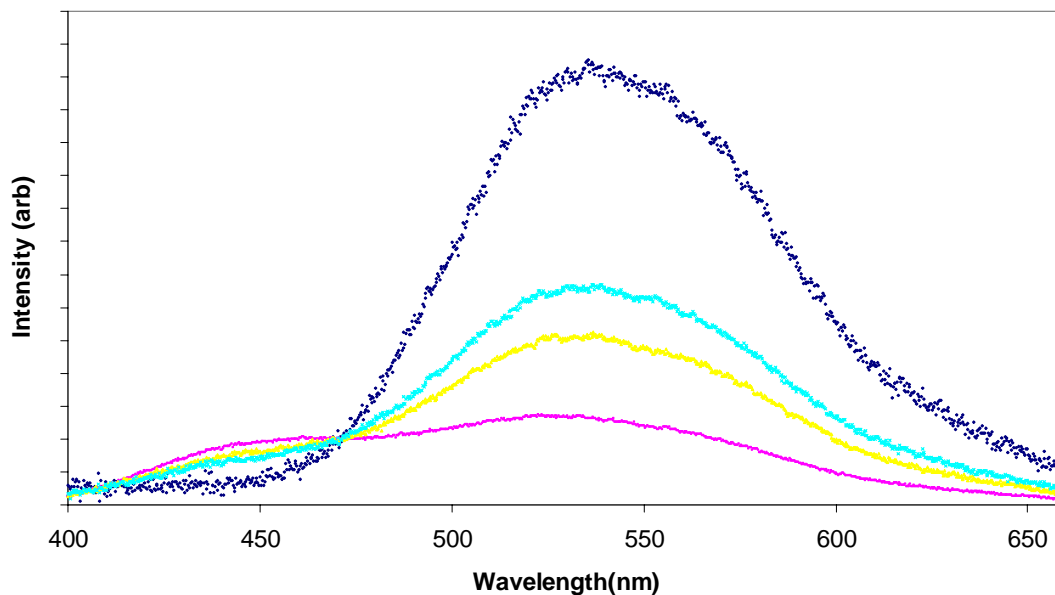


Figure 4.3. Fluorescent spectra of DND-160 in acetate at different pHs. Increasing peak at 540 nm corresponds to decreasing pH.

The spectra of DND-160 in an acetate buffer at different pH were shown in *Figure 4.3*. The spectra were normalized to its isosbestic point (470 nm). The fluorescence of DND-160 has two peaks at 440 nm and 530 nm. The peak at 440 nm diminishes at high pH. The fluorescence spectra response of the dye under high pressure tends to go to a low pH state of the dye; this spectral response is similar in all the buffer solutions used.

Since the dye of interest is a molecule with an intermolecular charge transfer, its fluorescence is highly dependent on solvent polarity^{20, 21}. The low pH fluorescence is similar in acetate, BES and MOPS while the high pH emission in acetate differs from the other two buffers (*Figure 4.4*). This difference may be due to difference in pKa of acetate compared to the other two (chemical structures is shown in *Figure 3.1*). At high pH, acetate was fully dissociated because the pKa was way below its pH while the other buffers were partially dissociated.

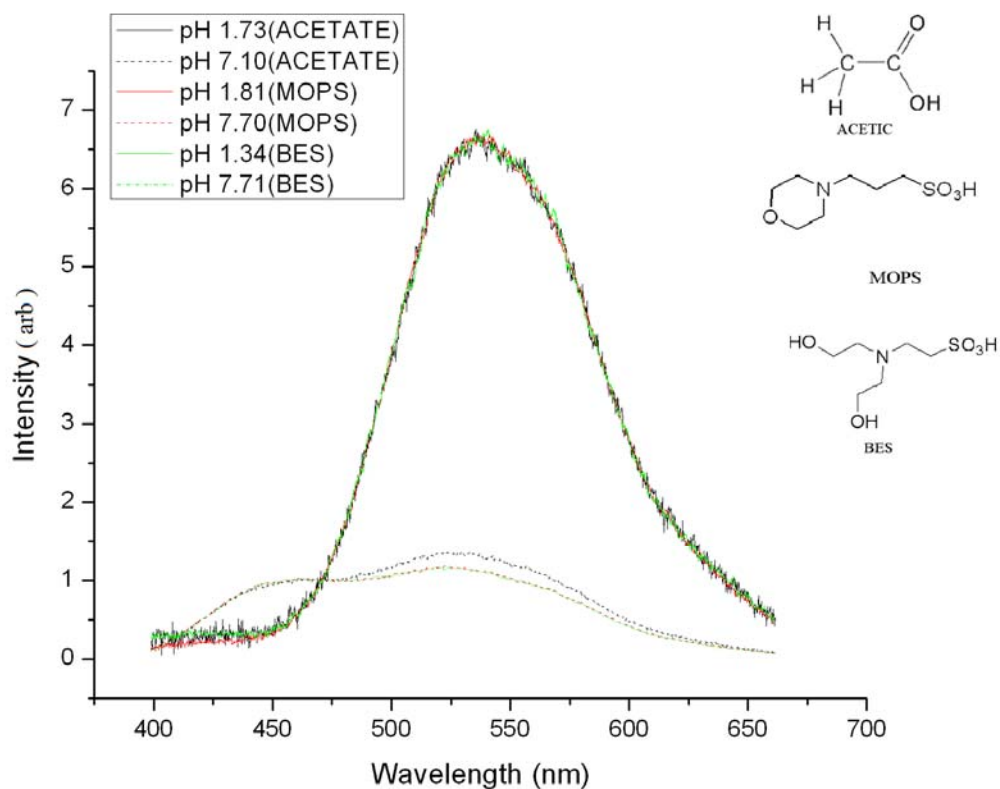


Figure 4.4. Fluorescent spectra of DND-160 in high and low pH

The pKa of DND-160 at 1 atm was determined using *Equation 2.4*. The resulting pKa values and the literature value for the pKa are shown in *Table 4.3*. As shown in the table, literature values for the apparent pKa has different values and basing on there result, DND-160's pKa has a linearly dependence on the excitation wavelength shown in *Figure 4.5*. Our pKa result with an excitation of 337 nm was in agreement with this dependence.

Table 4.3 pKa values of DND-160

Measured pKa (1 atm) ^d	Literature pKa
3.21 ± 0.004 (acetate)	4.47 ²⁰
2.98 ± 0.07 (MOPS)	3.5 _a ²⁸
3.11 ± 0.03 (BES)	4.0 _b ²⁸
	4.5 _c ²⁸

Excitation wavelengths: (a)350 nm, (b)365 nm,(c) 380 nm and (d)337 nm

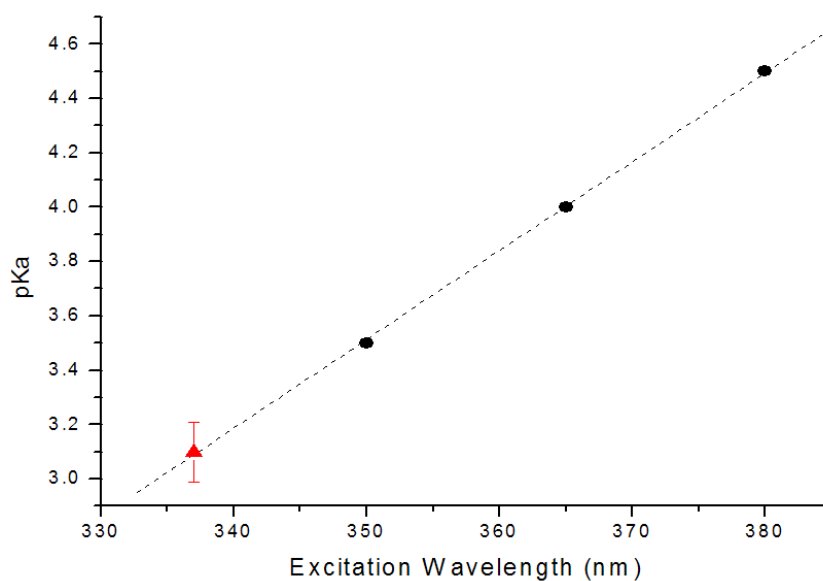


Figure 4.5. Excitation wavelength dependence of the pKa²⁸. The pKa value at 337 nm is the average of the measured pKa of DND-160 in acetate, MOPS and BES.

DND-160's high pH fluorescence is shown in *Figure 4.6*. The difference of the spectra between acetate and the Good's buffers can be seen at both the 1 atm and 512 atm fluorescence emissions. Also, the high pH emission peak redshifts as the pressure was increased from 1 atm to 512 atm, this is shown in *Figure 4.7*. The change of the intensity peaks at 1 atm and 512 was similar in all buffers used.

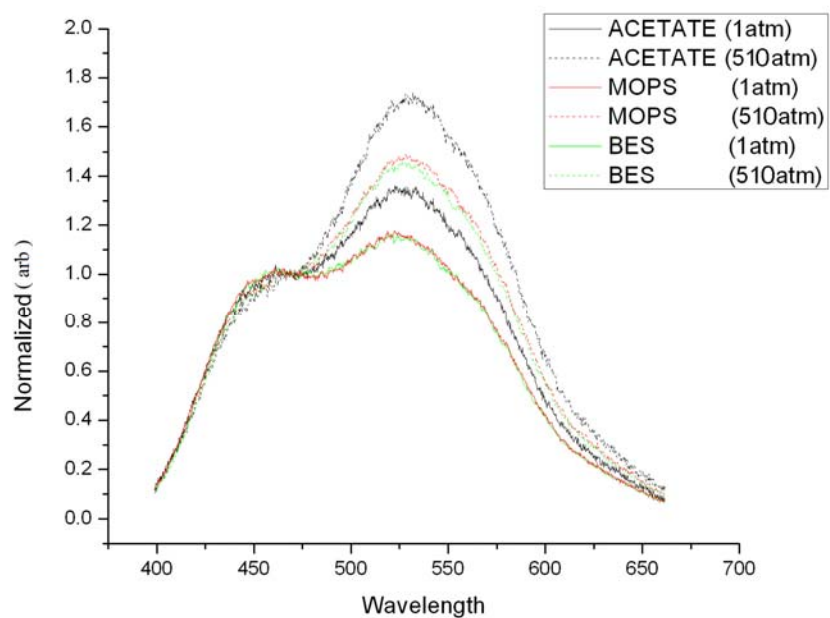


Figure 4.6. High pH Fluorescence emission at 1atm and 512atm

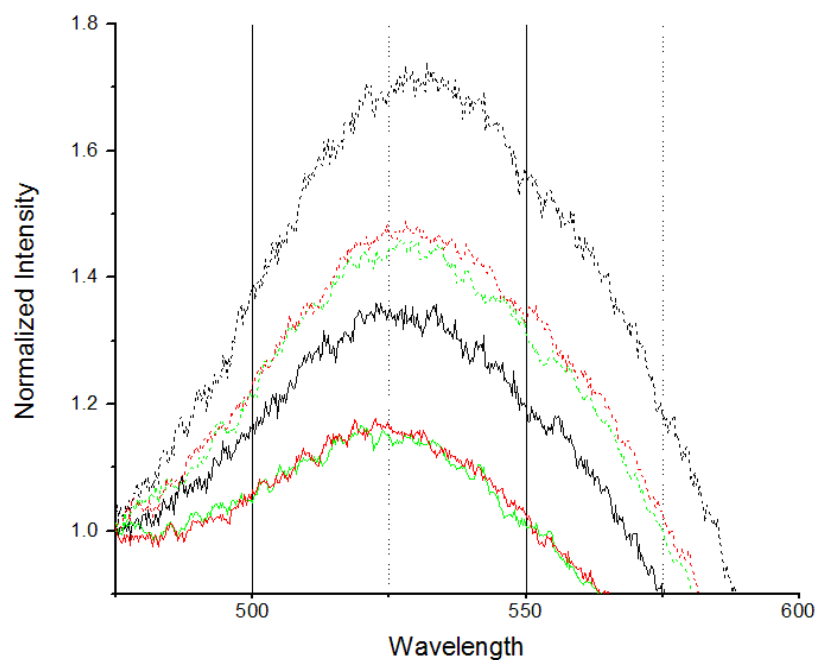


Figure 4.7. Pressure induced shift of the high pH emission peak

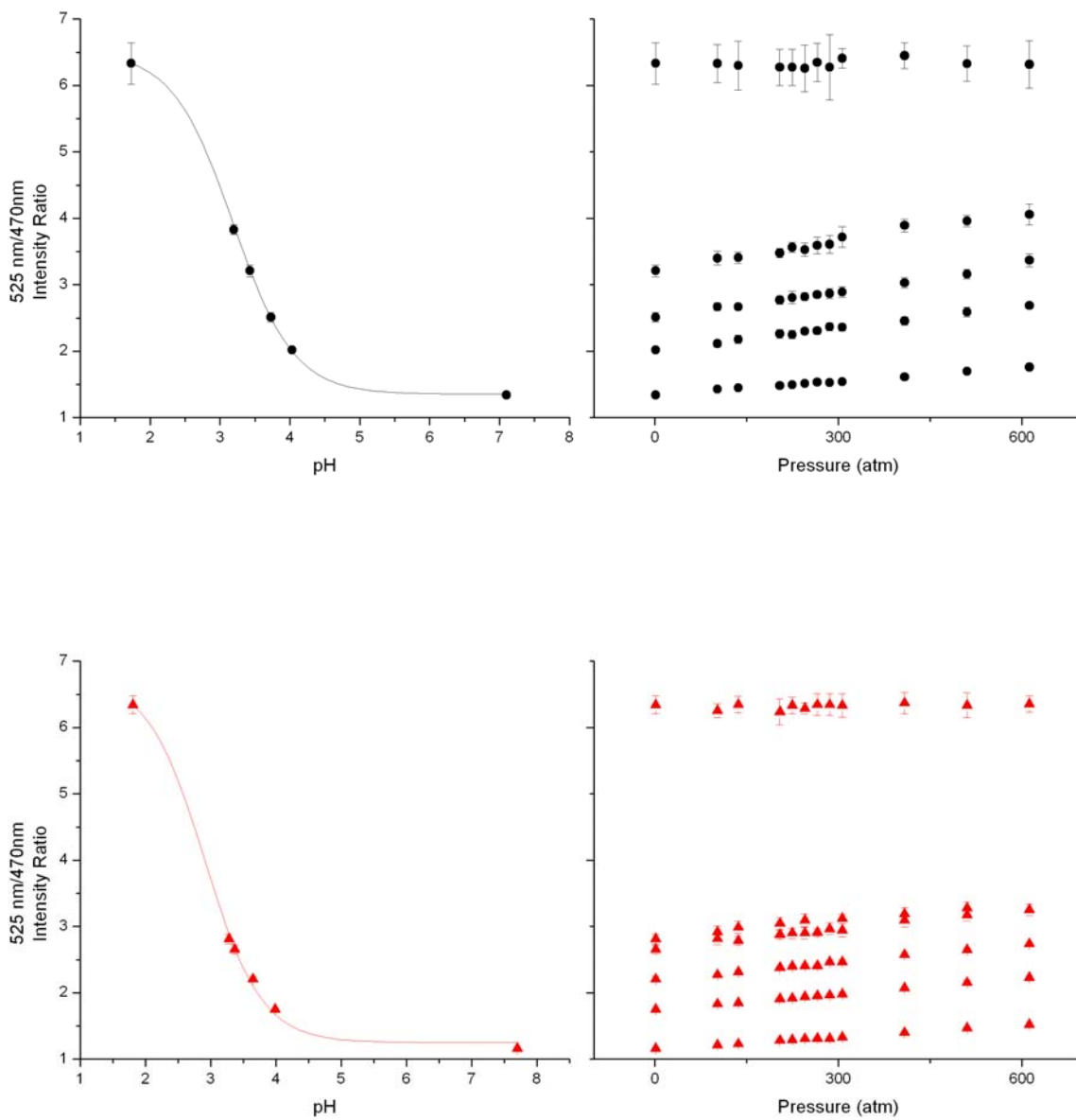


Figure 4.8.a Calibration curves at 1 atm and r(P) plots of DND-160 in acetate (top) and BES. The line in the calibration curve is a fit using *Equation 2.4*. The error bars are the standard deviation of 10 measurements.

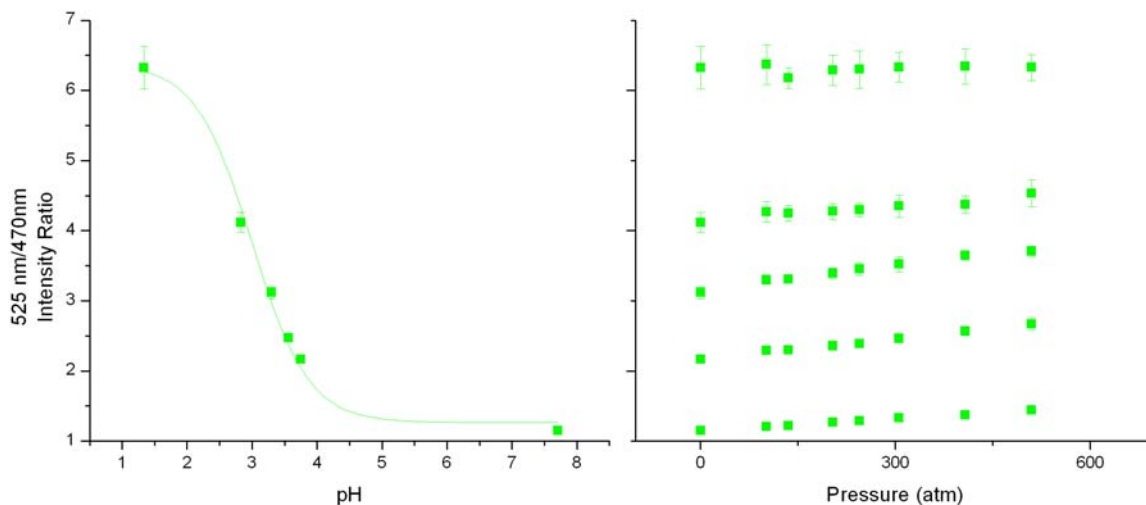


Figure 4.8.b Calibration curves at 1 atm and $r(P)$ plots of DND-160 in BES.

The calibration curve of DND-160 in acetate, MOPS and BES with the corresponding pressure responses of intensity ratio are shown in *Figure 4.8*. The low pH intensity ratios are constant under pressure. With increasing pressure, the r_{highpH} were changing. These results were consistent with all three buffers. This behavior of the high pH fluorescence of the DND-160 dye at different pressure is different from the C.SNAFL's and C.SNARF's dyes; the fluorescence of these dyes at their high and low pH forms was unchanged with changing pressure conditions. The intensity ratios response changes linearly with pressure. Also, the pressure responses of r_{highpH} in three buffers have similar slopes as shown in *Figure 4.10*. The calibration curve at 1 atm and 510 atm are shown in *Figure 4.9*. The calibration curve of DND-160 in MOPS and BES were similar at both pressures.

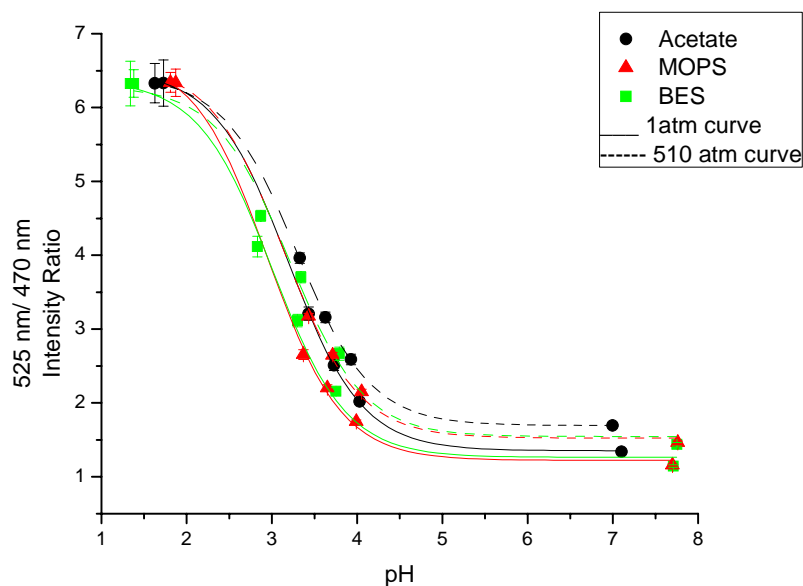


Figure 4.9. Calibration curve at 1 atm and 510 atm of DND-160 in acetate, MOPS and BES.

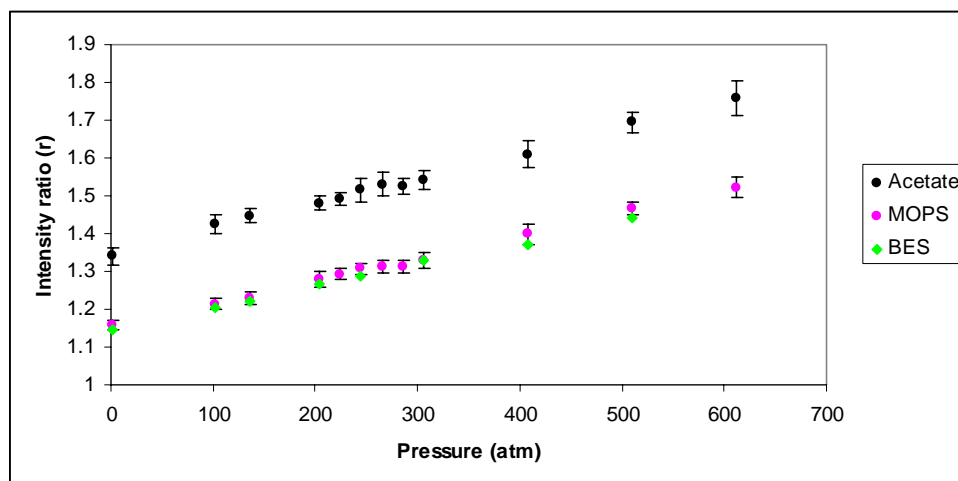


Figure 4.10. Pressure dependency of high pH intensity ratios

ΔV Calculations

The pressure dependent pK_a of the dye was determined using Eqn 2.4

$$pK_a(P) = pH(P) + \log \left[\frac{r - r_{highpH}}{r_{lowpH} - r} \times G \right],$$

with the values r_{lowpH} , r_{highpH} and the $pH(P)$ of the buffer used. The $pH(P)$ of the buffers were determined using *Eqn 2.5* and the buffer's ΔV .

$$pH(P) = pH(P_0) + \frac{1}{\ln 10} \frac{(P - P_0) \Delta V_{buffer}}{RT}$$

The corrected $pH(P)$ plots are shown in *Figure 4.11*. The buffers used were acetate (ΔV literature value is -11.2ml/mol), MOPS ($\Delta V = 7.06$ ml/mol), and BES ($\Delta V = 4.37$ ml/mol). The results show that DND-160 has a different ΔV_{dye} for acetate compared to MOPS and BES (*Table 4.4*).

Table 4.4. DND-160 ΔV_{dye} Results

Buffer used	ΔV_{dye} (ml/mol)
Acetate	9.63 ± 0.59
MOPS	18.59 ± 0.59
BES	19.4 ± 1.12

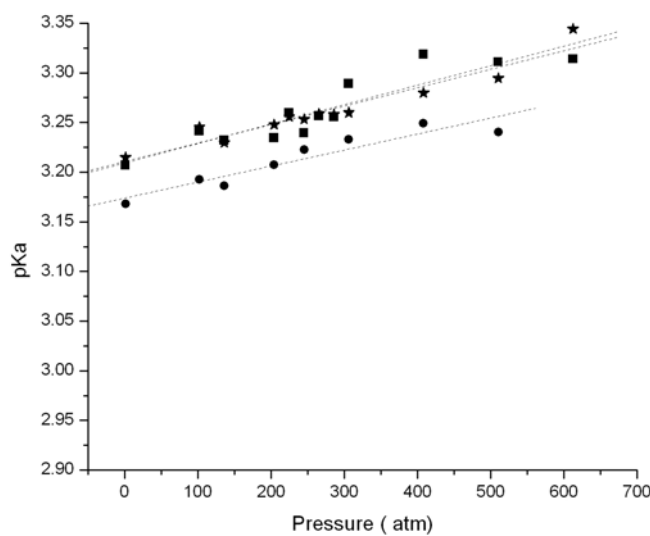


Figure 4.11.a $pK_a(P)$ of DND-160 in acetate. Fitted lines are fit to the data using *Eqn 2.6*.

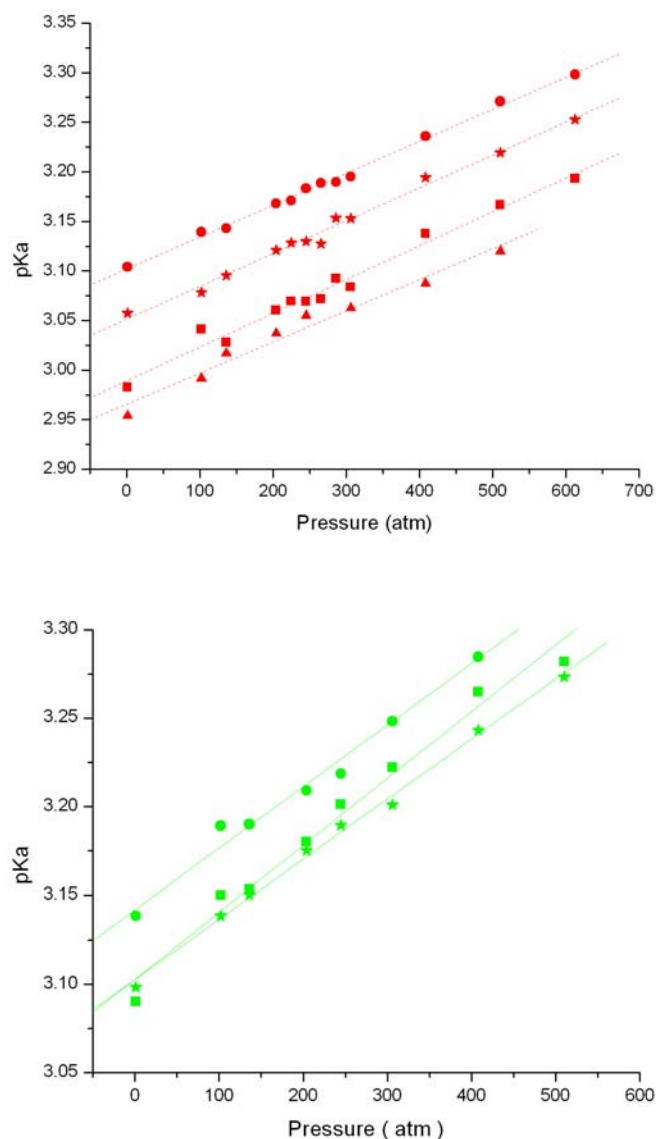


Figure 4.11.b. $pK_a(P)$ of DND-160 in MOPS and BES.

Discussions

Fluorescence of DND-160 is a result of an intramolecular charge transfer induced by the protonation of pyridine ring^{20, 28}. The charge transfer is between the pyridine and alkoxy group^{20, 21}. The fluorescence at low pH is due to the relaxation from the charge state (CT) while the emission from the deprotonated form is from the locally electronic (LE) excited state and

also the CT state. This can be seen from the emission of DND-160, at high pH two peaks are observed while there is only one emission peak at low pH. Since the emission of the protonated form is redshifted compared to the deprotonated form, the energy of the CT state is lower than the LE state (*Figure 4.12*)

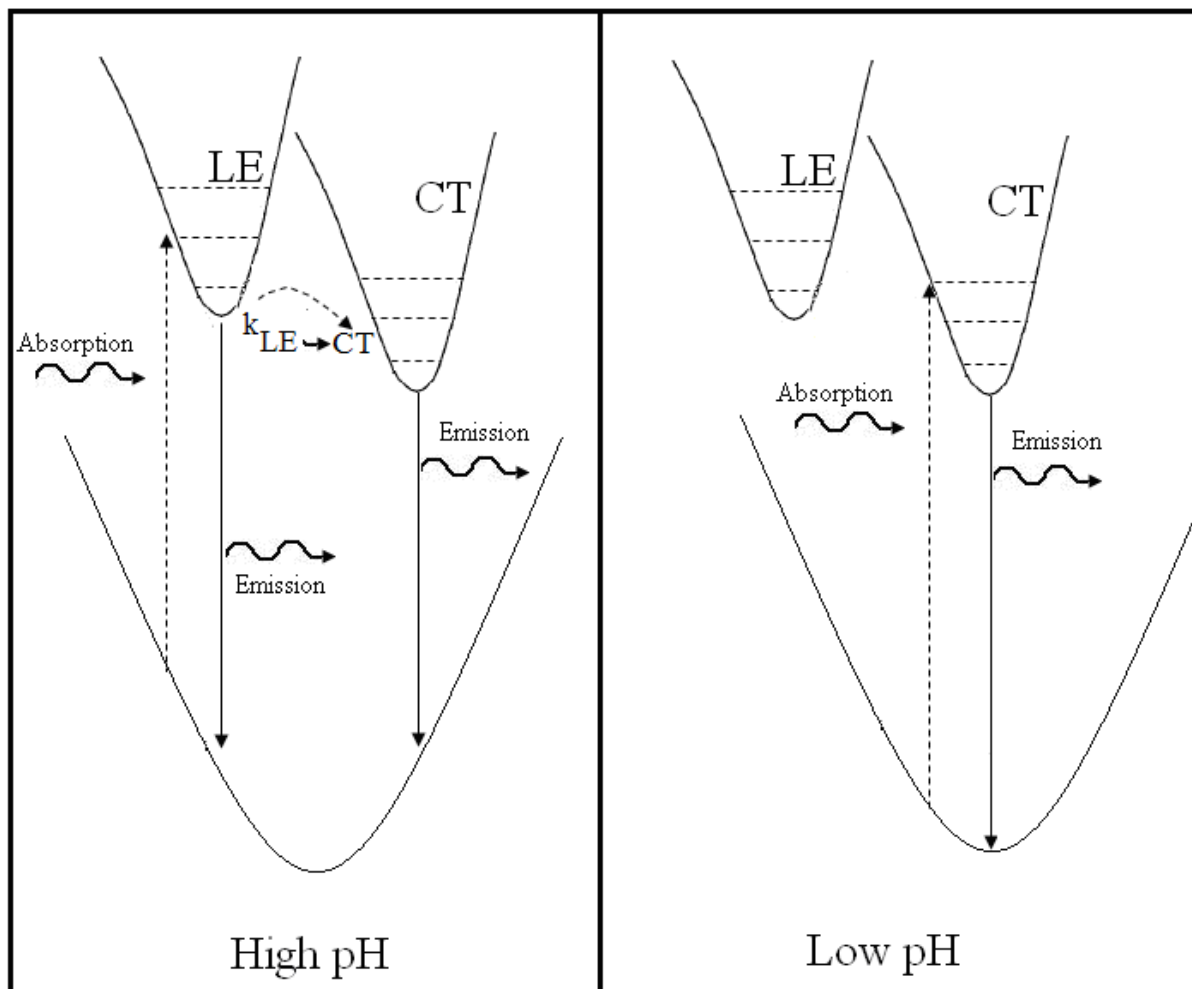


Figure 4.12. Single configuration coordinate model for intramolecular charge transfer molecules²². At high pH, fluorescence is due to relaxation of the excited state from the local electronic (LE) state and the charge state (CT) to the ground state. At low pH, absorption causes protonated form to excite to the charge transfer state, then eventually relaxing to the ground state.

In the pressure range of this thesis (1atm-600atm), high pH fluorescence shows some pressure dependence while there was no change for the low pH emission spectra. Also, the emission peak of the high pH form shifts during pressurization. Basing on the model proposed, this suggests

that the non-radiative transfer from the LE to CT state is pressure sensitive, this also true to the position of the CT state (see *Figure 4.13*). Also, the CT state at low pH is unchanged due to increasing pressure. This result suggests that protonation stabilizes the CT state. The mechanism of pressure dependence of the high pH form is that the non-radiative transfer from LE to CT state is changing under pressure and also the position of the CT state is also changing (see *Figure 4.13*). Possible causes for this change can be due to the change of solvent polarity (since solvent polarity change under pressure²⁹, or the change of the probe properties like its conformation (molecular twisting)^{23, 30}, or the change of the chemical equilibria of the dye.

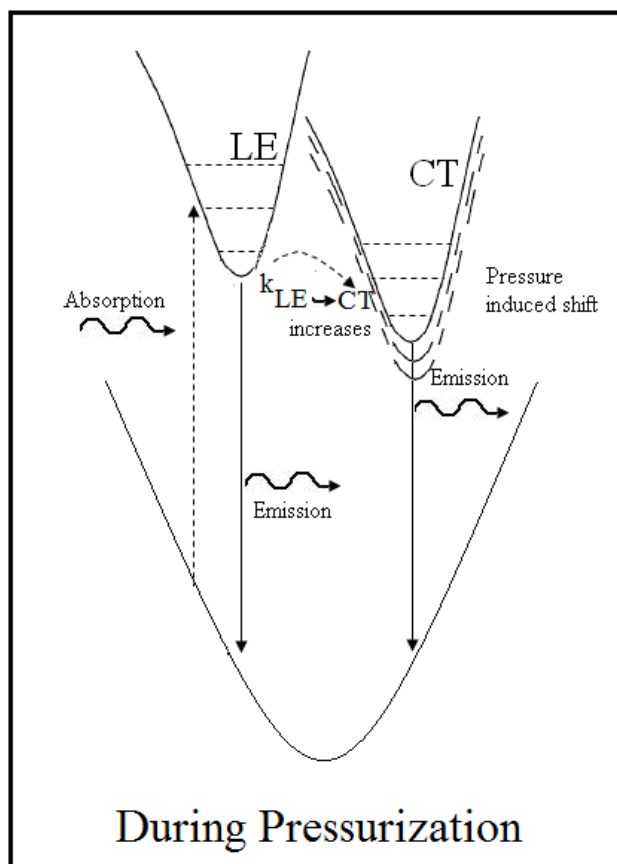


Figure 4.13. Scheme for pressure dependence of LE and CT states and their interaction. During pressurization, the nonradiative transfer rate increases and also the position of the CT state changes.

The fluorescence spectra of the high pH form under increasing pressure have some similar characteristics with all buffers. These similarities are the change of their intensities at 1 atm and 512 atm and also the slope of $r(P)$ (*Figures 4.7 and 4.10*). This means that the buffers used have

similar polarity. A large difference of solvent polarity of the buffers can make the fluorescence shift for both the high and low pH forms since the excited energy states of ICT molecules are dependent on solvent polarity²¹.

The ΔV_{dye} values found was different for acetate compared to BES and MOPS. The value for MOPS and BES is almost twice as the value for acetate. There can be a lot of reasons why they have different values. One of the reasons can be that the ΔV_{dye} measured is not the volume change of the chemical equilibria between the protonated[HD] and deprotonated[D] forms. This is an apparent ΔV_{dye} that is caused by the fluorescence characteristic of DND-160. The calculated ΔV_{dye} was based on the value of the shift of the equilibrium constant caused by pressurization. Also, the equilibrium constant was calculated from *Equation 2.6* which were based from equation 1.1 (Arrhenius relation) and from the interpretation of the measured intensity ratio. The intensity ratios were interpreted as the ratio of intensities that are based on the superposition of emissions of the two chemical forms of the dye, protonated and deprotonated forms. For the SNARF and SNAFL dyes, there fluorescence depends on the two fluorescent species of the dye, which are the protonated and the deprotonated form. Under increasing pressure, the chemical equilibria shifts to a system with lower volume, this also cause the change of the fluorescence spectra. For DND-160, its fluorescence depends on the protonated and deprotonated forms and also on the LE and CT states and there interactions. In order to get the real ΔV_{dye} , one must account the change of fluorescence other than the change of chemical equilibria. Even though the apparent ΔV_{dye} is not caused entirely by the fluorescence of the protonated and the deprotonated form, the two state model still fits (*Figure 4.9*)

Even though the apparent ΔV_{dye} is solvent dependent, this can still be used to correct the pH measured by DND-160 under high hydrostatic pressure. The value of the ΔV_{dye} was consistent for similar solvents like BES and MOPS but if its going to be used in other types of solution, it must be first calibrated in that solution under pressure in order for this dye, DND-160, to be used to measure accurate pH under pressure.

In summary, the fluorescence response of DND-160 under high hydrostatic pressure was different compared to pH sensing dyes C.SNAFLs and C.SNARFs. There difference is that DND-160 high pH fluorescence was pressure sensitive and its ΔV_{dye} was solvent dependent. This difference was due to the difference of the emission mechanism of DND-160 compared to C.SNAFL and C.SNARF.

CHAPTER V. CONCLUSIONS

Intracellular pH sensing under pressure requires a method of measuring pH accurately under this extreme condition. Using pH dyes for this type of pressure studies is much more convenient than using electric probes but pH sensing dyes need to be characterized under pressure for it to measure pH accurately under pressurization. In this thesis, a lysosomal pH probe, DND-160 was characterized under pressure. The specific goals of this thesis and their answers are written below:

- Can DND-160 be used as a low pH probe under high hydrostatic pressures?

Even with the difference of the results for DND-160 in comparison to the previously studied dyes, DND-160 can still be used under pressure. The apparent ΔV of DND-160 can be used as a correction factor for measuring pH under pressure (same method done on measuring pH(P) of buffers under pressure using C.SNAFL and C.SNARF). The only hindrance is that this ΔV is solvent dependent, which means characterization of DND-160 under pressure is needed for this dye to be used as a pH sensor for different solutions. For example, if DND-160 is used to measure lysosomal pH under high pressure, DND-160 must be characterized under high pressure in a solution that mimics lysosomal components^{8,31}.

- Given the different fluorescence mechanism of DND-160 compared to C.SNAFLs and C.SNARFs, what is the pressure dependence of DND-160 in different solutions?

The results for the effects of the fluorescence of DND-160 has some differences and similarities with a previous study done by Salerno, et al. on pH sensing dyes C.SNAFLs and C.SNARFs under high hydrostatic pressure. The comparison between this thesis and the Salerno et. al. study are listed below:

DIFFERENCES:

- The emission of the high pH form of DND-160 is pressure sensitive while for the pH dyes in the salerno study, the high pH dye's fluorescence were unchanged under pressure.
- The ΔV of DND-160 is solvent dependent. Its value is different in acetate and in pH buffers MOPS and BES; while in the salerno study, C.SNARF and C.SNAFL's ΔV was constant in different solvents.

SIMILARITIES

- The emission of the low pH forms of both DND-160 and pH dyes C.SNARF and C.SNAFL were pressure insensitive.
- The fluorescence of DND-160 and the pH dyes in the Salerno et. al. study follow the two state model. This two state model is based on a fluorescence mechanism which is due to the emission of the two forms of the dye (protonated and deprotonated form).
- What is a possible mechanism for this pressure dependence?

The differences of the fluorescence of the DND-160 and the dyes used in the Salerno study are due to the differences in there fluorescence mechanisms. C.SNAFL and C.SNARF's emission is solely dependent on the superposition of the fluorescence of its two dye forms: the protonated and deprotonated form; while for the DND-160's emission depends on two factors: the concentration of the two chemical forms (HD and D) and also on the interaction of its excited LE and CT state.

The mechanism proposed for the fluorescence of DND-160 in this thesis is that the emission of the low pH form is due to the dual fluorescence coming from the charge transfer (CT) state

and locally electronic (LE) state, while at high pH the fluorescence is coming from the CT state.. During pressurization, low pH fluorescence change due to the increase of the non-radiative rate ($k_{LE \rightarrow CT}$), which makes the emission due to CT to increase. This mechanism is inspired by the previously studied fluorescent dyes PRODAN and ADMA²². The main focus for this thesis is not to verify this mechanism but to show that high pressure use for DND-160 is possible. One way to verify this model is by doing a lifetime measurement of the fluorescence of DND-160, these would be the same experiment describe in Rollinson et. al.²². The model tells us that expression for the time dependent intensity, $I(t)$, is a double exponential decay,

$$I(t) = A_1 e^{-\frac{t}{\tau_1}} + A_2 e^{-\frac{t}{\tau_2}}$$

where τ_1 and τ_2 are the lifetime due to emission from the LE and CT state respectively. Since the CT state is being fed from the LE state, the time dependent intensity due to the CT emission can be expressed in terms of the nonradiative transfer $k_{LE \rightarrow CT}$. During pressurization, the value of $k_{LE \rightarrow CT}$ will increase according to the model proposed. This result could also vary due to the fact that in this model, only one way of nonradiative transfer is possible, which is $k_{LE \rightarrow CT}$. It's also a possibility that excited state molecule in the LE or CT state could relax to the ground state nonradiatively. Also, one interesting value to look at when doing these lifetime measurement is the lifetime due to CT emissions at high and low pHs, since there is a peak difference between CT emissions at low and high pHs.

s

REFERENCES

- 1 F. Abe, "Exploration of the effects of high hydrostatic pressure on microbial growth, physiology and survival: Perspectives from piezophysiology," *Bioscience Biotechnology and Biochemistry* 71 (10), 2347-2357 (2007).
- 2 M. D. Basson *et al.*, "Effects of increased ambient pressure on colon cancer cell adhesion," *Journal of Cellular Biochemistry*. 78 (1), 47-61 (2000).
- 3 P. Manas and B. M. Mackey, "Morphological and physiological changes induced by high hydrostatic pressure in exponential- and stationary-phase cells of *Escherichia coli*: Relationship with cell death," *Applied and Environmental Microbiology*. 70 (3), 1545-1554 (2004).
- 4 R. J. St John, J. F. Carpenter and T. W. Randolph, "High pressure fosters protein refolding from aggregates at high concentrations," *Proceedings of the National Academy of Sciences of the United States of America*. 96 (23), 13029-13033 (1999).
- 5 D. A. Lown, H. R. Thirsk and Wynnejon.L, "Effect of Pressure on Ionization Equilibria in Water at 25 Degrees C," *Transactions of the Faraday Society* 64 (548P), 2073-& (1968).
- 6 A. Drljaca *et al.*, "Activation and reaction volumes in solution. 3," *Chemical Reviews* 98 (6), 2167-2289 (1998).
- 7 P. Chan, J. Lovric and J. Warwicker, "Subcellular pH and predicted pH-dependent features of proteins," *Proteomics* 6 (12), 3494-3501 (2006).
- 8 N. Demaurex and S. Grinstein, "Organelle pH homeostasis and proton conductances," *Journal of Physiology-London* 527, 15S-16S (2000).
- 9 N. Demaurex, "pH homeostasis of cellular organelles," *News in Physiological Sciences* 17, 1-5 (2002).

- 10 B. Dale *et al.*, "Intracellular pH regulation in the human oocyte," *Human Reproduction* 13 (4), 964-970 (1998).
- 11 J. M. Holopainen *et al.*, "Elevated lysosomal pH in neuronal ceroid lipofuscinoses (NCLs)," *European Journal of Biochemistry* 268 (22), 5851-5856 (2001).
- 12 Y. Q. Miao, J. R. Chen and K. M. Fang, "New technology for the detection of pH," *Journal of Biochemical and Biophysical Methods* 63 (1), 1-9 (2005).
- 13 A. Roos and W. F. Boron, "Intracellular pH," *Physiological Reviews*. 61 (2), 296-434 (1981).
- 14 A. S. Yang and B. Honig, "On the pH-dependence of Protein Stability," *Journal of Molecular Biology*. 231 (2), 459-474 (1993).
- 15 V. V. Khramtsov, "Biological imaging and spectroscopy of pH," *Current Organic Chemistry* 9 (9), 909-923 (2005).
- 16 Joseph P. Lakowicz, *Principles of Fluorescence Spectroscopy*, 3rd Edition, 2006 .
- 17 F. Abe and K. Horikoshi, "Analysis of intracellular pH in the yeast *Saccharomyces cerevisiae* under elevated hydrostatic pressure: a study in baro- (piezo-) physiology," *Extremophiles* 2 (3), 223-228 (1998).
- 18 R. J. Quinlan and G. D. Reinhart, "Baroresistant buffer mixtures for biochemical analyses," *Analytical Biochemistry*. 341 (1), 69-76 (2005).
- 19 M. Salerno *et al.*, "Characterization of dual-wavelength seminaphthofluorescein and seminaphthorhodafluor dyes for pH sensing under high hydrostatic pressures," *Analytical Biochemistry*. 362 (2), 258-267 (2007).
- 20 Z. J. Diwu *et al.*, "A novel acidotropic pH indicator and its potential application in labeling acidic organelles of live cells," *Chemistry and Biology*. 6 (7), 411-418 (1999).

- 21 Z. Diwu *et al.*, "Fluorescent molecular probes .2. The synthesis, spectral properties and use of fluorescent solvatochromic Dapoxyl(TM) dyes," *Journal of Photochemistry and Photobiology A - Chemistry* . 66 (4), 424-431 (1997).
- 22 A. M. Rollinson and H. G. Drickamer, "High-Pressure study of Luminescence from Intramolecular CT Compounds," *Journal of Chemical Physics*. 73 (12), 5981-5996 (1980).
- 23 H. G. Drickamer, "High-Pressure Studies of Molecular Luminescence," *Annual Review Phys.Chem.* 33, 25-47 (1982).
- 24 Z. Diwu *et al.*, "Fluorescent molecular probes .2. The synthesis, spectral properties and use of fluorescent solvatochromic Dapoxyl(TM) dyes," *Journal of Photochemistry and Photobiology A - Chemistry*. 66 (4), 424-431 (1997).
- 25 M. Salerno *et al.*, "Characterization of dual-wavelength seminaphthofluorescein and seminaphthorhodafluor dyes for pH sensing under high hydrostatic pressures," *Analytical Biochemistry* (2), 258-267 (2007).
- 26 J. J. Ajimo, "A UV-Visible-NIR, Time-Resolved Fluorescence Spectrometer for High-Pressure Biological Studies," Masters Thesis, Department of Physics, Miami University (2005).
- 27 E. C. Raber *et al.*, "Capillary-based, high-pressure chamber for fluorescence microscopy imaging," *Review of Scientific Instruments*. 77 (9), (2006).
- 28 H. J. Lin *et al.*, "Fluorescence lifetime characterization of novel low-pH probes," *Analytical Biochemistry*. 294 (2), 118-125 (2001).
- 29 W. B. Floriano and M. A. C. Nascimento, "Dielectric constant and density of water as a function of pressure at constant temperature," *Brazilian Journal of Physics* 34 (1), 38-41 (2004).

- 30 Z. R. Grabowski *et al.*, "Twisted Intra-molecular Charge-Transfer States (TICT) - New Class of Excited-States with a Full Charge Separation," *Nouveau Journal De Chimie-New Journal of Chemistry* 3 (7), 443-454 (1979).
- 31 E. C. Dell'Angelica *et al.*, "Lysosome-related organelles," *Faseb Journal* 14 (10), 1265-1278 (2000).